METHODOLOGY OF IDENTIFYING SUPER-CYCLES IN SILVER PRICES

A THESIS SUBMITTED TO
THE GRADUATE SCHOOL OF NATURAL AND APPLIED SCIENCES
OF
MIDDLE EAST TECHNICAL UNIVERSITY

BY

TUĞBA SOYSAL

IN PARTIAL FULFILLMENT OF THE REQUIREMENTS
FOR
THE DEGREE OF MASTER OF SCIENCE
IN
STATISTICS

AUGUST 2023

Approval of the thesis:

METHODOLOGY OF IDENTIFYING SUPER-CYCLES IN SILVER PRICES

submitted by **TUĞBA SOYSAL** in partial fulfillment of the requirements for the degree of **Master of Science in Statistics Department, Middle East Technical University** by,

Prof. Dr. Halil Kalıpçılar _____
Dean, Graduate School of **Natural and Applied Sciences**

Prof. Dr. Özlem İlk Dağ _____
Head of Department, **Statistics**

Assoc. Prof. Dr. Ceren Vardar Acar _____
Supervisor, **Department of Statistics**

Examining Committee Members:

Prof. Dr. Vilda Purutçuoğlu
Statistics Dept., METU _____

Assoc. Prof. Dr. Ceren Vardar Acar
Statistics Dept., METU _____

Prof. Dr. İbrahim Ünalmış
Economi & Finance Dept., Bahçeşehir University _____

Date: 29.08.2023

I hereby declare that all information in this document has been obtained and presented in accordance with academic rules and ethical conduct. I also declare that, as required by these rules and conduct, I have fully cited and referenced all material and results that are not original to this work.

Name, Last Name: TUĞBA SOYSAL

Signature :

ABSTRACT

METHODOLOGY OF IDENTIFYING SUPER-CYCLES IN SILVER PRICES

Soysal, Tuğba
M.S., Department of Statistics
Supervisor : Assoc. Prof. Dr. Ceren Vardar Acar

August 2023, 66 pages

Silver is mainly used in industry and it also has started to attract attention as an investment tool in recent years. In periods of economic expansion and increased industrial activity, there is a tendency for the demand for silver to rise, which might push prices higher. Contrarily, economic downturns or financial c rises m ay l imit i ndustrial demand for silver and cause prices to decline.

This thesis aims to provide important insights into the potential upward gains and downward losses and the time required for the super-cycle to end. To do that the highest possible increase and also the highest possible drop in silver prices are estimated, and the duration of the cycle is examined. The highest possible increase means the highest possible gain in finance. Conversely, the highest possible drop means the highest possible loss. The study used the concept of super-cycles, that consist of both upward and downward movements in the price series, to pinpoint the data point with the maximum gain or maximum loss in the silver price covering the year 2005 and 2023. These super-cycles were extracted using the Hodrick Prescott economic filter-

ing approach by excluding the trend components and smoothing the data. Fractional Brownian motion model is used to simulate silver prices. The fBm is selected because it is considered realistic due to its ability to portray long-term dependent behavior. In the end of this study, simulation results which indicate the expected duration of the super-cycle are presented.

Keywords: Silver Prices, Maximum Drawup, Maximum Drawdown, Fractional Brownian Motion, Super-cycles, Hodrick Prescott Filter

ÖZ

GÜMÜŞ FİYATLARINDA SÜPER DÖNGÜLERİ BELİRLEME YÖNTEMİ

Soysal, Tuğba
Yüksek Lisans, İstatistik Bölümü
Tez Yöneticisi : Doç. Dr. Ceren Vardar Acar

Ağustos 2023, 66 sayfa

Ağırlıklı olarak sanayide kullanılan gümüş, son yıllarda bir yatırım aracı olarak da ilgi görmeye başlamıştır. Ekonomik genişleme ve artan endüstriyel faaliyet dönemlerinde, gümüş talebinin artma eğilimi vardır ve bu da fiyatların yükselmesine neden olabilir. Aksine, ekonomik gerilemeler veya finansal krizler endüstriyel gümüş talebini sınırlayabilir ve fiyatların düşmesine neden olabilir.

Bu tez, potansiyel yukarı yönlü kazançlar ve aşağı yönlü kayıpları ve süper döngünün tamamlanması için gerekli süreyi hesaplamak hakkında önemli bilgiler sağlamayı amaçlamaktadır. Bunun için gümüş fiyatlarındaki olası en yüksek artış ve ayrıca olası en yüksek düşüş tahmin edilir ve süper döngünün süresi incelenir. Mümkün olan en yüksek artış, finansta mümkün olan en yüksek kazanç anlamına gelir. Buna karşılık, mümkün olan en yüksek düşüş ise en yüksek zarar anlamındadır. Bu çalışmada, 2005 ve 2023 yıllarını kapsayan gümüş fiyatındaki olası en yüksek artışın ve en yüksek düşüşün olduğu veri noktasını belirlemek için fiyat serilerindeki hem yukarı hem de

aşağı hareketlerden oluşan süper döngüler kavramı kullanıldı. Hodrick Prescott ekonomik filtreleme yaklaşımı ile trend bileşenleri hariç tutuldu ve verileri yumuşatıldı. Gümüş fiyatlarını simüle etmek için kesirli Brownian hareket modeli kullanıldı. Kesirli Brownian hareketi, uzun vadeli bağımlı davranışı tasvir etme yeteneği nedeniyle gerçekçi olduğu için seçilmiştir. Bu çalışmanın sonunda, gümüş datasının süper döngünün beklenen süresini gösteren simülasyon sonuçları sunulmuştur.

Anahtar Kelimeler: Gümüş Fiyatları, Maksimum Kazanç, Maksimum Kayıp, Süper Döngüler, Kesirli Brown Hareketi, Uzun Dönemli Çevrimler, Hodrick Prescott Filtresi

To my family

ACKNOWLEDGEMENTS

I sincerely thank my supervisor, Assoc. Prof. Dr. Ceren Vardar Acar for her wise counsel and encouragement as I worked to complete this master's thesis. Her knowledge and suggestions were quite helpful in determining the course of the study. I am grateful to her for her kindness and the environment of cooperation she provided.

To my husband and best friend, Mustafa Soysal, your constant support and understanding has been my light. Your words of support during challenging times and your joy even in my smallest successes have meant the world to me.

I would like to express my gratitude to my dear friend Berna İpek. Her motivational and supportive remarks have been a major factor in helping me stay focused and committed to achieving my objectives throughout my master's thesis work.

I also want to express my heartfelt gratitude to my family, for their endless trust in my abilities.

TABLE OF CONTENTS

ABSTRACT v

ÖZ vii

ACKNOWLEDGEMENTS x

TABLE OF CONTENTS xi

LIST OF TABLES xiv

LIST OF FIGURES xvi

LIST OF ABBREVIATIONS xvii

CHAPTERS

1 INTRODUCTION 1

1.1 Introduction 1

2 HIGHEST POSSIBLE INCREASE AND HIGHEST POSSIBLE DROP 7

2.1 Fractional Brownian Motion 7

2.1.1 Properties 9

2.2 Duration of the Highest Possible Increase and Drop 13

3 SUPER-CYCLES AND HODRICK-PRESCOTT FILTERING TECHNIQUE 17

3.1 Super-cycles 17

3.2 Data and Filtering Methods 19

3.2.1 Hodrick-Prescott Filter 20

4 MODELING, ESTIMATION AND SIMULATION 23

4.1 Modeling using fBm 23

4.1.1 Stochastic Model 23

4.2 Assumption Check of fBm for Silver Prices 28

4.2.1 Normality 28

4.2.2 Stationarity 31

4.2.3 Dependency 33

4.3 Estimation of H 35

4.4 Simulation 37

4.5 The Model Validation 43

5 CONCLUSION 45

REFERENCES 49

APPENDICES

A TABLES OF TIME SERIES 55

LIST OF TABLES

TABLES

Table 3.1 Value of the Smoothness Parameter 21

Table 4.1 KPSS Test Results of $\ln(S_t) - \ln(S_{t-1})$ 32

Table 4.2 ADF Test Results of $\ln(S_t) - \ln(S_0)$ 33

Table 4.3 Estimates of Hurst Parameter and 95 percent CIs 36

Table 4.4 Comparison of the Simulation Study with the Actual Data Set for t=222, Hurst Parameter=0.732 41

Table 4.5 The Highest Possible Drop Simulation for t=222, Hurst Parameter=0.732 42

Table 4.6 The Mean Square Errors 44

Table A.1 Hodrick-Prescott Filtering Results 55

Table A.2 Hodrick-Prescott Filtering Results-Cont. 56

Table A.3 Hodrick-Prescott Filtering Results-Cont. 57

Table A.4 Hodrick-Prescott Filtering Results-Cont. 58

Table A.5 Hodrick-Prescott Filtering Results-Cont. 59

Table A.6 Hodrick-Prescott Filtering Results-Cont. 60

Table A.7 Hodrick-Prescott Filtering Results-Cont. 61

Table A.8 Hodrick-Prescott Filtering Results-Cont. 62

Table A.9 Hodrick-Prescott Filtering Results-Cont. 63

Table A.10 Hodrick-Prescott Filtering Results-Cont. 64

Table A.11 Hodrick-Prescott Filtering Results-Cont. 65

Table A.12 Hodrick-Prescott Filtering Results-Cont. 66

LIST OF FIGURES

FIGURES

Figure 1.1 Silver Price Data: World Bank 3

Figure 3.1 Phases of the Business Cycle 19

Figure 4.1 Initial Histogram of Standardized Log-returns of the Silver Prices (Z^1 - Z^2) 29

Figure 4.2 Points Applied HP Filter in Silver Price Data 30

Figure 4.3 Final Histogram of Standardized Log-returns of the Silver Prices (Z^1 - Z^2) 30

Figure 4.4 Correlation Diagrams 34

Figure 5.1 Silver Price Data: World Bank 47

LIST OF ABBREVIATIONS

Bm	Brownian Motion
fBm	Fractional Brownian Motion
GfBm	Geometric Fractional Brownian Motion
HP	Hodrick Prescott
ACF	Autocorrelation Function
PACF	Partial Autocorrelation Function
KPSS	Kwiatkowski-Phillips-Schmidt-Shin
ADF	Augmented Dickey Fuller

CHAPTER 1

INTRODUCTION

1.1 Introduction

Researchers, investors, and politicians have all shown a keen interest in the study of commodity prices and how they relate to the overall economy. Due to high volatility and widespread contagion in financial markets, investors have sought alternative investment instruments as a means of diversifying their portfolios and mitigating the increasing risk in stock markets. In this context, oil and major precious metals like gold, palladium, platinum, and silver have emerged as desirable asset classes for portfolio diversification. These assets exhibit different volatilities and returns, and they demonstrate lower correlations with stocks, both at the sector and market levels [33]. For making wise investment choices and controlling financial risks, it is essential to comprehend how commodity prices are affected by prevailing economic conditions and other important factors.

Silver occupies a prominent position in the world commodities market due to its numerous uses in industry, the creation of jewellery, and demand for investments. As a result, a wide range of variables, such as macroeconomic indicators, dynamics of supply and demand, investor attitude, and geopolitical developments, have an impact on silver prices.

One significant factor affecting silver prices is the state of the global economy. The demand for silver can be affected by factors in the economy like GDP expansion, inflation rates, interest rates, and currency fluctuations. The demand for silver tends

to increase during times of economic growth and heightened industrial activity, which could put upward pressure on prices. In contrast, economic downturns or financial crises may stifle demand from industry for silver and lower prices.

Commodity prices are significantly influenced by supply and demand dynamics in addition to macroeconomic factors [42]. According to Nguyen and Walther (2020), the amount of global real economic activity, as well as shifts in consumer sentiment, industrial production, and economic policy uncertainty, all have a substantial impact on long-term volatility [13]. They also discover that the Industrial Production has a detrimental effect on the long-term volatility of Gold and Silver[42].

This thesis aims to give useful insights whether the last super-cycle of silver prices ended or not and about the duration of that cycle. With this aim we will find the highest possible increase and the highest possible decrease and durations of these amounts. A determination of the size of significant price increases or decreases can be made by analyzing historical data, which also provides information about the viability of upward trends. These results contribute to a deeper comprehension of the silver investment dynamics and risk-return characteristics. The data set used is World Bank Commodity Markets Silver prices.

Data

The data set on silver prices from the World Bank's commodity markets is suitable for this study.[1] The World Bank is a reputable international organisation which is well-known for its thorough and accurate data. The data set covers a sizable amount of time in monthly frequency from January 2005 to June 2023. With this prolonged time frame, it is possible to conduct a thorough examination of silver prices that takes into account varied market circumstances and economic cycles.

By analysing the long-range dependence of silver price data, researchers can gain insights into patterns and changes over time, and potentially develop more accurate data models.

[1] Monthly silver prices in nominal US dollars/troy oz is taken from the World Bank website www.worldbank.org/en/research/commodity-markets.

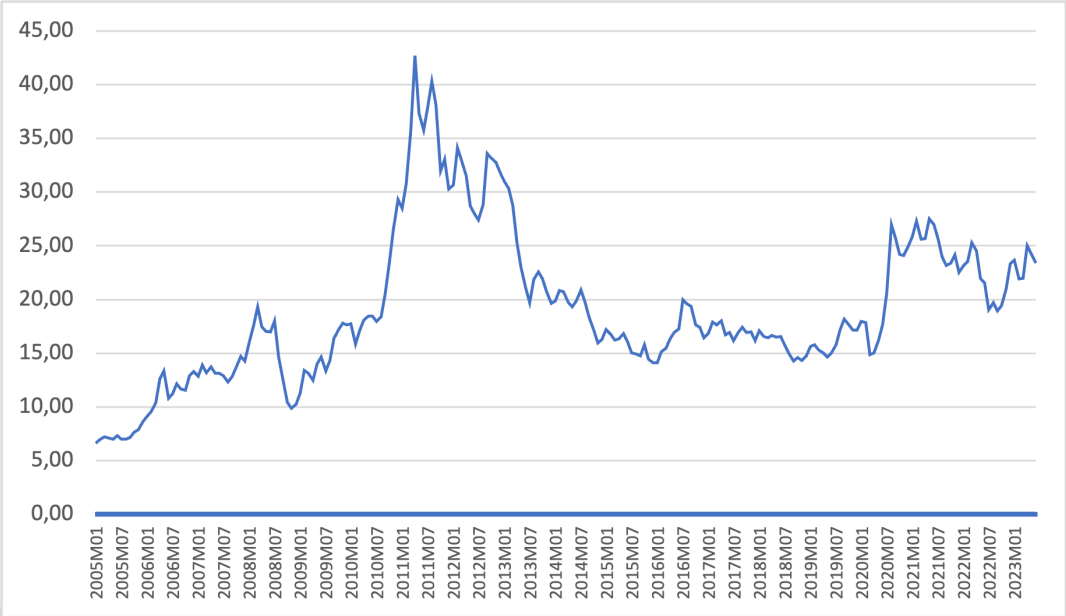


Figure 1.1: Silver Price Data: World Bank

In our study, to analyse the silver price data using the fractional Brownian motion (fBm), the monthly returns are computed first by taking the percentage change in price between consecutive months and compared to starting value as well. The resulting time series were then analysed using fBm model assumptions. Silver price modeling is carried out using an exponential Black-Scholes model with fBm.

We prefer a probabilistic model as fBm rather than using a time series model. Time series models are good to forecast for short time spans. Whereas in our study we work with long period data and probabilistic models work better in such data.

The definition of the geometric fBm uses the exponential of the increments of a fractional Brownian motion rather than the increments of a Brownian motion.

We utilize process $S(t)$, which is the solution of the stochastic differential equation which is driven by fBm, to represent the price of silver at time t:

$$dS(t) = \mu S(t)dt + \sigma S(t)dB^H(t) \tag{1.1}$$

where $S(0) = s$, constant mean μ and constant volatility σ are higher than 0, $B^H(t)$ stands for fractional Brownian motion. The Hurst parameter is used to identify fractional Brownian motion. The Hurst parameter serves as a defining characteristic of

fBm, which exhibits long- or short-term dependency as well as self-similarity features. The Hurst parameter is the "index of dependence" that connects the model to the time series' autocorrelations.

The validity of the fractional Brownian motion model and its suitability for capturing the properties of the silver data must be confirmed through normality, stationarity and dependency assumptions. Checking for normality is determining if the logarithm variations in silver prices are distributed normally. We used tools like histograms and the Jarque-Bera test to verify normality. Examining the stationarity of increments means determining if the statistical characteristics of the time series data stay constant throughout the course of time. KPSS and ADF tests helped us to identify the stationarity in our data set. We also determined if there is a long-term dependency in price returns. This involves examining autocorrelation and estimating the Hurst exponent, which shows the degree of dependency in the data.

The remaining part of this masters thesis is organised as follows. The second chapter, which also introduces and defines fBm, will detail the highest possible increase and highest possible drop and also duration of these. In finance, highest possible increase, often known as maximum gain, refers to the largest possible market gain. In contrary, highest possible drop means the highest possible loss from peak to through. As a result, both of them are crucial for economists and investors as well. In order to pinpoint the highest silver price peak together with the highest silver price drop and allow us to focus just on the relevant evidence, super-cycles will be discussed in Chapter 3.

Super-cycles are characterized by consecutive upward and downward motion. The economic filtering method that super-cycles employ to obtain data from the series is covered in this section. The filtering method used in this study is the Hodrick Prescott filter. The data may be smoothed and the trend component of the series can be separated from the series using this filtering technique. It is possible to recognize the most recent super-cycle using the Hodrick Prescott filter. Beginning of the most recent super-cycle is the initial data point taken into account for modeling.

Whether the silver price data meet the criteria of the stochastic differential equation described in Equation 1.1 will be explored in Chapter 4 along with the feasibility of this model. The assumptions are checked using tests for normality, stationarity, and dependency. In the same section, the conclusions based on each assumption are provided. The Hurst parameter (H) will be computed to convince that Equation 1.1 can be used as a model for our data set. Then, in order to evaluate our simulation codes for producing fBm, we will perform simulations to ascertain the expected highest possible increase and drop of Brownian Motion. In the final chapter, simulation results with a real-world data collection will be compared and the depth of the maximum increase/drop in silver prices will be approximated and analyzed.

CHAPTER 2

HIGHEST POSSIBLE INCREASE AND HIGHEST POSSIBLE DROP

2.1 Fractional Brownian Motion

Mathematician Benoit Mandelbrot and physicist John W. Van Ness initially proposed fractional Brownian motion (fBm) in 1968 as a generalization of the traditional Brownian motion process. Mandelbrot, widely credited as the creator of fractal geometry, was drawn to the idea of creating a mathematical model that could account for the long-range correlations and self-similarity seen in a variety of natural phenomena, including the shapes of coastlines, cloud formations, and stock price changes.

The standard Brownian motion, a random walk process that is intended to simulate the movement of particles in a fluid or gas, is utilized to create the fBm process. The outcome is a continuous-time stochastic process that displays self-similarity over several time scales, or the ability to maintain its identity under various magnifications. One of the shortcomings of a Brownian motion model, however, is that the increments are independent. Fractional Brownian motion, on the other hand, enables to model incremental dependencies in asset prices [6][44]. The fractional Brownian motion, by definition, has dependent increments and thus captures the dependency properties of real-life data, such as market returns.

The time series models are data driven models and hence generally they compare the statistical properties of the current cycle with the previous cycles in the data set and reach a conclusion about whether the current cycle has ended or not. And such an interpretation would be specific to the analyzed data set. The studies [38] and [14]

suggest wavelet-based stochastic models capture probabilistic properties of processes since they are able to discuss the features of cycles from a broader perspective considering all possible paths rather than focusing only on the current data set. With time series it is not possible to undertake whether a cycle ended or not as it only estimates the next short term development in the data. And, one of the well known wavelet based continuous time stochastic model is fractional Brownian motion. Fractional Brownian motion also captures and explains the self similarity property of the real market prices.

Studies that evaluated the effectiveness of fBm-based models to other conventional models in diverse applications have been conducted. In a research by Pospisil and Kritoufek [37], for instance, they evaluated the performance of fBm-based models with autoregressive integrated moving average (ARIMA) models in predicting stock prices and discovered that the fBm-based models offered superior predictions over longer time horizons.

The performance of fBm-based models and ARIMA models in simulating the volatility of the Istanbul Stock Exchange (ISE) National 100 Index was also compared in a study by Eryigit and Guliyev [17], who discovered that the fBm-based models offered a better fit to the data and generated more precise volatility forecasts.

In multiple disciplines, including finance, economics, physics, and engineering, fBm has many uses. Modelling financial time series data, which frequently displays long-term dependency and non-normal distributions, makes use of it particularly well.

Fractional Brownian motion is described by Mandelbrot and Van Ness as an integral with regard to standard Brownian motion, which has a fractional parameter $Hin(0, 1)$. Harold Edwin Hurst [27], who studied the water level in the Nile River, developed this parameter, which is known as the Hurst parameter. The Hurst exponent (H) establishes the degree of long-term dependency in the data, and is used in fBm to describe the process. A positive shock is more likely to be followed by a negative shock and vice versa when the Hurst exponent is less than 0.5, which is when the process exhibits anti-persistence. When the Hurst exponent exceeds 0.5, it is more

likely that a positive shock will be followed by another positive shock and vice versa. The process transforms into a simple Brownian motion when the Hurst exponent is equal to 0.5.

2.1.1 Properties

Definition 2.1.1 *Let $(\Omega, \mathcal{F}, \boldsymbol{P})$ be a probability space and let H be a constant in the interval $(0, 1)$. fBm, $B^H(t)$, with Hurst parameter H, is a continuous, Gaussian process with zero mean and has this covariance function ($t \geq 0$) [4]:*

$$Cov_H(t) = E[B^H(t)B^H(s)] = \frac{1}{2}(t^{2H} + s^{2H} - |t-s|^{2H}).$$

Standard Brownian motion is represented by fBm for $H = 1/2$ [4], where the covariance function becomes:

$$E[B^{1/2}(s)B^{1/2}(t)] = \frac{1}{2}(t + s - |t-s|) = min(t, s)$$

Fractional Brownian motion $B^H(t)$ has the following properties:

1. Assume $B^H(0) = 0$ and $E[B^H(t)] = 0$ for all $t \geq 0$.
2. B^H has homogeneous increments, i.e., $B^H(t+s) - B^H(s)$ has the same law of $B^H(t)$ for $s, t \geq 0$.
3. B^H is a Gaussian process and $E[B^H(t)^2] = t^{2H}$, $t \geq 0$, for all $H \in (0, 1)$.
4. B^H has continuous trajectories.

Correlation between two increments The procedure becomes standard Bm and has independent increments when H parameter is set to 1/2. The fBm procedure, however, has dependent increments when $H \neq 1/2$. The covariance for the two processes may be determined from the fBm's definition. The covariance of the increments

$B^H(t+h) - B^H(t)$ and $B^H(s+t) - B^H(s)$ with $s+h \leq t$ and $t-s = nh$ is

$$\begin{aligned}
&\rho_H(n) = E[((B^H(t+h) - B^H(t))(B^H(s+h) - B^H(s)))] \\
&= E[B^H(t+h)B^H(s+h)] - E[B^H(t+h)B^H(s)] \\
&- E[(B^H(t))B^H(s+h)] + E[B^H(t)B^H(s)] \\
&= \frac{1}{2}[((t+h)^{2H} + (s+h)^{2H} - |(t+h) - (s+h)|^{2H}) \\
&- ((t+h)^{2H} + s^{2H} - |(t+h) - s|^{2H}) \\
&- (t^{2H} + (s+h)^{2H} - |t - (s+h)|^{2H}) \\
&+ (t^{2H} + s^{2H} - |t-s|^{2H})] \\
&= \frac{1}{2}[-2(t-s)^{2H} + (t-s-h)^{2H} + (t-s+h)^{2H}] \\
&= \frac{1}{2}[-2(nh)^{2H} + ((n-1)h)^{2H} + ((n+1)h)^{2H}]
\end{aligned} \tag{2.1}$$

So we have

$$E[((B^H(t+h)-B^H(t))(B^H(s+h)-B^H(s)))] = \frac{h^{2H}}{2}[(n+1)^{2H}+(n-1)^{2H}-2n^{2H}]$$

Given that fBm is a Gaussian process, its mean and covariance structure are distinct. However, the presence of dependent increments might lead someone to question the stationarity of fBm. If the unconditional joint probability distribution remains unchanged over time, a stochastic process is said to be stationary. The following example illustrates how the stationarity property works:

$$\begin{aligned}
&E[((B^H(t+h) - B^H(h))(B^H(s+h) - B^H(h)))] = \\
&E[B^H(t+h)B^H(s+h)] - E[B^H(t+h)B^H(h)] \\
&- E[(B^H(h))B^H(s+h)] + E[B^H(h)^2] \\
&= \frac{1}{2}[((t+h)^{2H} + (s+h)^{2H} - |(t+h) - (s+h)|^{2H}) \\
&- ((t+h)^{2H} + h^{2H} - |(t+h) - h|^{2H}) \\
&- (h^{2H} + (s+h)^{2H} - |h - (s+h)|^{2H}) \\
&+ (h^{2H} + h^{2H} - |h-h|^{2H})] \\
&= \frac{1}{2}[t^{2H} + s^{2H} + |t-s|^{2H}] \\
&= E[B^H(t)B^H(s)]
\end{aligned} \tag{2.2}$$

Therefore, for the fBm if the Hurst exponent remains the same over time, there is stationarity in the process.

Long-range dependence

Definition 2.1.2 *Assume that* $(Y_n)_{n\in N}$ *is a stationary time series and it is the long-range dependent. This process' covariance* $\rho(n) := Cov(Y_k, Y_{k+n})$ $(Y_n)_{n\in N}$ *is in accordance with:*

$$\lim_{n\to\infty} \frac{\rho(n)}{cn^{-\alpha}} = 1$$

where c *is a constant and* $\alpha \in (0, 1)$. *[4]*

In a long-range dependent process, as n rises, the dependence between $Y_k + n$ and Y_k eventually decreases as:

$$\sum_{n=1}^{\infty} \rho(n) = \infty$$

With the use of the covariance function, it turns out that fBm demonstrates the long-range dependency behavior. The correlation among the increments is as follows:

$$\begin{aligned} \rho_H(n) :&= E[(B^H(t+h) - B^H(t))(B^H(s+h) - B^H(s))] \\ &= \frac{h^{2H}}{2}[(n+1)^{2H} + (n-1)^{2H} - 2n^{2H}] \end{aligned} \tag{2.3}$$

Applying the expansions provided below;

$$(1+x)^{\alpha} = 1 + \alpha x + \frac{\alpha(\alpha-1)x^2}{2} + ...$$

$$(1-x)^{\alpha} = 1 - \alpha x + \frac{\alpha(\alpha-1)x^2}{2} - ...$$

covariance develops:

$$\begin{aligned} \rho_H(n) &= 1 + 2H\frac{1}{n} + \frac{2H(2H-1)}{2}\frac{1}{n^2} + 1 - 2H\frac{1}{n} + \frac{2H(2H-1)}{2}\frac{1}{n^2} + ... \\ &\cong \frac{n^H}{2}(2H(2H-1))\frac{1}{n^2} \\ &= H(2H-1)n^{2H-2} \end{aligned} \tag{2.4}$$

According to the Definition 2.1.2, c equals to $H(2H-1)$ and α equals to $2-2H$. Therefore, for $H > 1/2$ the process has the property of long-range dependence because

The Definition of 2.1.2 states that $c = H(2H-1)$ and $\alpha = 2-2H$. The process bears the attribute of long-range dependency for $H > 1/2$ as a result.

$$\lim_{n\to\infty} \frac{\rho_H(n)}{H(2H-1)n^{2H-2}} = 1. \tag{2.5}$$

In conclusion, we get

1. For $H > 1/2$, $\sum_{n=1}^{\infty} \rho_H(n) = \infty$.
2. For $H < 1/2$, $\sum_{n=1}^{\infty} |\rho_H(n)| < \infty$.

We may deduce that the two increments $B^H(t+h) - B^H(t)$ and $B^H(t+2h) - B^H(t+h)$ have a positive correlation if $H > 1/2$. On the other hand, these two increments exhibit a negative connection with $H < 1/2$. Long-range dependence is a crucial and the most significant characteristic for analyzing the long-term behavior in the financial data. The correlation diagram is an effective way to represent this characteristic.

The Self-similarity property

Definition 2.1.3 *The real-values process $Y_t, t \geq 0$ is self-similar if there is a $b > 0$ such that for every $a > 0$*

$$(Y_{at})_{t>0} \overset{law}{=} (bY_t)_{t\geq 0}.$$

This indicates that the finite-dimensional distributions of $Y_{at}, t \geq 0$, and $bY_t, t \geq 0$ are equivalent; in other words, if for every option to $t_0, ..., t_n$ and any $a \geq 0$, respectively,

$$(Y_{at_1}, Y_{at_2}, ..., Y_{at_n}) \overset{d}{=} (bY_{t_1}, bY_{t_2}, ..., bY_{t_n}). \tag{2.6}$$

It may be inferred that the process $Y_t, t \geq 0$ *satisfies the self-similarity condition if* $b = a^H$ *in Equation 2.6.[4].*

For $H = 1/2$*, The Standard Brownian Motion's self-similarity feature is rediscovered as* $(B(a^{1/2}t))_{t>0} \overset{law}{=} (a^{1/2}B(t))_{t\geq 0}$.

We may utilize the distribution of a self-similar process across a unit interval to infer the distribution of the process throughout the entire time interval since scaling in time interestingly coincides with scaling in space.

2.2 Duration of the Highest Possible Increase and Drop

Financial data typically has a lot of descents and ascents in it. One of the variations in the data set that has to be examined is the highest possible increase. In the context of financial analysis, highest possible increase refers to the highest rise in value that a portfolio or investment has ever seen over a given time period, from its lowest point to its highest position. Essentially, it is the inverse of highest possible drop, also known as maximum loss, indicates the highest possible market risk in finance.

The highest possible increase has a variety of uses. First of all, it enables investors to evaluate an investment strategy's or portfolio's potential upward move or growth. Investors can estimate the highest level of return they might have been able to realize over a particular time period by studying the expected highest possible increase. The highest possible increase can also be used to assess the effectiveness of investment strategies. It gives an indication of how well-positioned a portfolio or investment is to profit from market upswings.

The highest possible increase can be utilized in risk decision-making procedures. Investors can acquire a thorough knowledge of the risk return profile of an investment by looking at both the highest possible increase and drop. By using this information, asset allocation decisions may be made that balance the need to manage negative risks while also capturing possible rewards. The ratio of the expected gain to expected risk could be used to struct portfolios.

Inspired by these applications in statistics, mathematical finance and risk theory, there has been an increasing interest in the study of the maximum loss/drawdown/gain/-drawup of the fBm defined as below.

Notation: The fractional Brownian motion is denoted by the symbol $B^H(t)$. Then, the formula for highest possible increase before time t is given as

$$\begin{aligned} M_t^{H,+} :&= \sup_{0\le u\le v\le t}(B_v^H - B_u^H) \\ &= \sup_{0\le v\le t}((B_v^H - \inf_{0\le u\le v} B_u^H) - B_u^H) \\ &:= \sup_{0\le v\le t} D_v^{H,+} \end{aligned} \tag{2.7}$$

where the process's gain or drawup is denoted by the constant $D_t^{H,+}$. The appropriate highest possible increase duration for M_t^H for some $M > 0$ may be defined as

$$\begin{aligned} E(M_t^{H,+}) &= E(\sup_{0\le u\le v\le t}(B_v^H - B_u^H)) \\ &= E(\sup_{0\le \frac{u}{t}\le \frac{v}{t}\le 1}(B_v^H - B_u^H)) \\ &= E(\sup_{0\le u'\le v'\le 1}(B_{v't}^H - B_{u't}^H)) \\ &= E(\sup_{0\le u'\le v'\le 1} t^H(B_{v'}^H - B_{u'}^H)) \\ &= t^H E(\sup_{0\le u'\le v'\le 1} t^H(B_{v'}^H - B_{u'}^H)) = t^H E(M_1^{H,+}) \end{aligned} \tag{2.8}$$

by the self similarity property of fBm.

Following is the notation of the highest possible drop. Let $B^H(t)$ denote the fractional Brownian motion. Then, the mathematical definition of maximum loss before time t is given as

$$\begin{aligned} M_t^{H,-} :&= \sup_{0\le u\le v\le t}(B_u^H - B_v^H) \\ &= \sup_{0\le v\le t}((\sup_{0\le u\le v} B_u^H) - B_v^H) \\ &:= \sup_{0<v<t} D_t^{H,-} \end{aligned} \tag{2.9}$$

where $D_t^{H,-}$ is called the loss or the drawdown of the process. For M_t^H for some

$M > 0$, the corresponding the duration of the highest possbile drop can be defined as

$$\begin{aligned} E(M_t^{H,-}) &= E(\sup_{0\le u\le v\le t}(B_u^H - B_v^H)) \\ &= E(\sup_{0\le \frac{u}{t}\le \frac{v}{t}\le 1}(B_u^H - B_v^H)) \\ &= E(\sup_{0\le u'\le v'\le 1}(B_{u't}^H - B_{v't}^H)) \\ &= E(\sup_{0\le u'\le v'\le 1} t^H(B_{u'}^H - B_{v'}^H)) \\ &= t^H E(\sup_{0\le u'\le v'\le 1} t^H(B_{u'}^H - B_{v'}^H)) = t^H E(M_1^{H,-}) \end{aligned} \tag{2.10}$$

by the self similarity property of fBm.

Now suppose $M_t^{H,+} = m$ for some $m > 0$. Let $H_m^{D,+} = \inf(t \ge 0; D_t^{H,+} = m)$ and let $\rho = \sup(t \in [0, H_m^{D,+}]; D_t^{H,+} = 0)$. Then the duration of highest possible increase is defined as:

$$\begin{aligned} \tau_m &:= H_m^{D,+} - \rho \\ &= \inf(t \ge 0; D_t^H = m) - \sup(t \in [0, H_m^D]; D_t^H = 0) \end{aligned} \tag{2.11}$$

This thesis proposes an approach to model silver prices. By doing this we aim to predict the duration of super-cycle through the highest possible increase and drop and average duration of these amounts. In order to determine the greatest gain and its length in time, we must first set the beginning point or level of silver price fluctuations for our estimating study. The following chapter discusses the start of the most recent super-cycle, which have the longest durations and most variability. This cycle included the last excursion at the greatest height. Additionally, access to the highest possible increase and its length is truly made available by the excursion under running supremum with the greatest height.

CHAPTER 3

SUPER-CYCLES AND HODRICK-PRESCOTT FILTERING TECHNIQUE

In this chapter, we discuss filtering techniques as well as the concept and classification of super-cycles. We first define the period for our historical data analysis and then use the statistical model to calculate the highest possible increase. By examining the super-cycles, we can determine this time frame. There have been multiple super-cycles up to this time. We'll concentrate on the most recent cycle.

3.1 Super-cycles

Super-cycles are long-lasting increases in commodity prices that can endure for decades or even centuries. In a super-cycle, there is a strong demand for commodities, which causes prices to remain high for an extended length of time. This may be the result of a number of things, including fast industrialization, population expansion, technical development, and changes in trade regulations.

Throughout history, super-cycles have been seen in the commodities markets. For instance, a super-cycle in commodities like copper, rubber, and tin occurred in the late 19th and early 20th centuries as a result of increasing demand brought on by the industrial revolution. Another instance is the super-cycle in commodity prices that occurred from the late 1990s to the middle of the 2010s, which was fueled by demand from developing nations like China and India.

Because it may shed light on the long-term patterns and factors influencing commodity prices, the notion of super-cycles is crucial for understanding the dynamics of

commodity markets. Additionally, it can assist policymakers and investors in better anticipating and controlling the risks related to changes in commodity prices.

The term "business cycle" describes the cyclical fluctuations in the economy that are marked by contractions (times of economic downturn or recession) and expansions (times of economic growth) [24]. Typically, these cycles involve adjustments to indicators like the GDP, job levels, investments, consumer spending, and industrial production.

Market economies naturally and regularly experience business cycles, which are impacted by a variety of variables including changes in technology, monetary and fiscal policy, and world events. To effectively manage risks and opportunities in the economy, politicians, investors, and companies must have a thorough understanding of the patterns and dynamics of economic cycles.

Thomas Palley (2011) [36] divides economic cycles into three categories:

Inventory cycles **:** These are short-term, less than a year-long cycles that result from changes in inventory levels. Factors including customer demand, production costs, and loan accessibility have an impact on inventory cycles.

Business cycles **:** These medium-term cycles, which generally span two to 10 years, are marked by changes in economic activity. Interest rate fluctuations, alterations in governmental regulations, and changes in the state of the global economy all have an impact on business cycles.

Long waves **:** These are cycles that persist for a very long time—a century or more. Technological progress, alterations in the population, and shifts in the global power structure all have an impact on long waves. Kondratieff waves are another name for these cycles.

The stages of the business cycle are depicted in Figure 3.1. An entire business cycle, including two peak points and one trough, may be seen from one peak to the next. A business cycle's length might range from a few months to several years. For economists and investors, it is essential to comprehend and forecast these cycles.

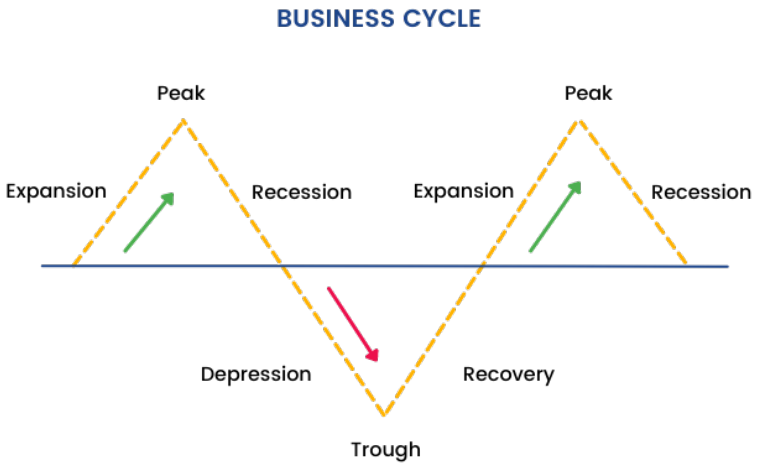


Figure 3.1: Phases of the Business Cycle

To understand how well and how efficiently an economy is performing, economists study business cycles. They can determine if the economy is experiencing growth or decline by recognizing the business cycle phase. Economic decisions and policies are influenced by this information.

There is no agreement on the exact starting date of the last super cycle in the literature. 1996, 1998 and early 2000s are possible starting dates mentioned [15] [16]. We have taken 2005 as the starting date in our analysis.

An economic filter is used on the silver data to determine the cyclical fluctuations. The cycle is extracted using this filter by detrending and smoothing [34]. Then, detrended data can be examined to spot changes in the business cycle. We will only apply Hodrick-Prescott filter to our data set.

3.2 Data and Filtering Methods

Working with silver data provides valuable insights into the dynamics of the commodities markets with market trends, supply and demand dynamics. It also gives insights on portfolio diversification with clarifying risk-return profile. Additionally, it contributes to evaluate the economic health by being a hedge against inflation. Given its usage in a variety of industries, including electronics, solar energy, and medical

equipment, silver data also offers visibility into industry demand. Moreover, it helps with risk management by reducing supply chain interruptions and price volatility. With all these, analyzing silver data offers useful knowledge for academics, politicians, investors, and sectors that depend on silver.

Economic filters are commonly used to identify cycles in economic time series data. By removing the cyclical component from the initial time series, these filters enable us to identify the underlying business cycle.

One of the most used filters, the Hodrick-Prescott (HP) filter, separates a time series into a trend component and a cyclical component [26]. The cyclical component depicts the short-term variations around the trend, whereas the trend component indicates the time series' long-term behaviour.

3.2.1 Hodrick-Prescott Filter

The Hodrick-Prescott filter is the filtering method we applied in our study. Macroeconomic specialists overwhelmingly choose this filter for detrending and smoothing, according to Nilsson and Gyomai (2011) [34]. The Hodrick-Prescott (HP) filter is a commonly used technique to decompose a time series in to a trend component and a cyclical component. By reducing the overall variations in the data, the filter divides a time series into two pieces, a long-term trend and a short-term cycle.

The HP filter penalizes the trend's curvature and estimates the trend component as the smoothest function that can fit the data. A parameter, which regulates the level of smoothing and establishes the trade-off between fitting the data and smoothing the trend, sets the penalty.

The cyclical component is then calculated using the difference between the original time series and the estimated trend component.

The Hodrick-Prescott (HP) filter's smoothness parameter λ value controls how much smoothing is applied to the data. A smoother trend line is produced by a higher value of λ, whereas a more volatile trend line is produced by a lower value of λ. The precise

Table 3.1: Value of the Smoothness Parameter

frequency	λ
annual	100
quarter	1600
monthly	14400

properties of the data being analyzed and the analysis's objectives determine the right value of λ.

$$Y_t = T_t + c_t$$

$$min_{T_t} \sum_t (Y_t - T_t)^2 + \lambda \sum_t \left[(T_{t+1} - T_t)(T_t + T_{t-1}) \right]^2$$

where the actual time series is represented by Y_t, the trend component by T_t, the cyclical component by c_t, and the smoothing parameter by λ [34].

The minimizing between the trend and cyclical component is provided by λ. The smoothing parameter λ should be set before applying the filter. As noted in Table 3.1, the variable λ only accepts positive values; typically, it equals 100 for yearly data and 14400 for monthly data as stated in [39].

In this study, the HP filter was applied using the Excel hp-filter component. Our data was gathered on a monthly basis, hence the smoothness parameter's value, λ, is 14400.

CHAPTER 4

MODELING, ESTIMATION AND SIMULATION

4.1 Modeling using fBm

The price of financial instruments is frequently modeled using the Black-Scholes model, which makes the assumption that geometric Brownian motion exists. In this model, it is presumed that the price of the underlying asset would increase in distinct phases, which suggests that the price changes are independent of one another [8]. This presumption might not apply to actual financial data because prices frequently show long-range dependency and clustering of volatility.

In such cases, the adoption of the Black-Scholes model with fBm may be more suitable than the classic Black-Scholes model for capturing dependent behavior in financial data. In addition to capturing the persistent behavior frequently seen in financial time series, fBm enables the modeling of processes with memory [19].

4.1.1 Stochastic Model

The stochastic Geometric Brownian motion (GBm) model is commonly used in option pricing [5] and stock price modeling [40]. The GBm model considers independent and normally distributed stock returns. It has been widely used to simulate stock price paths in numerous studies and has demonstrated alignment with actual prices.

The GBm model has been used to explain the randomness seen in commodity prices in a couple studies. In a research with gold [50], the future price path for gold prices

in Malaysia was shown using geometric Brownian motion. GBm was also utilized to forecast the iron ores and it is stated that GBm method is a good tool to aid in reducing investment risks and uncertainties [2]. However, the primary discrepancy between empirical study on actual data, which predominantly exhibits dependence known as self-similarity or long memory, and GBm modeling is that it implies that real stock increments are mutually independent [3]. The Geometric Fractional Brownian Motion (GfBm) was created to overcome this restriction by adding the Hurst exponent into the stock price dynamics [3]. By revealing details regarding the degree of self-similarity present in a particular time series, this improvement seeks to increase the accuracy of stock price modeling. Financial data is frequently used in GfBm approach [32]. The GfBm methodology has also been applied to other disciplines, such as hydrology [18] and information technology [46][47].

In our study, our main interest is to estimate whether or not the last super cycle is completed therefore, without the loss of generality, we use the silver prices smoothed at values where there are jumps or outliers. This consideration implies that the components of the jumps in the stochastic continuous-time model might be ignored. The GfBm model which fits the estimation of silver prices is as follows:

$$dS(t) = \mu S(t)dt + \sigma S(t)dB^H(t) \tag{4.1}$$

where $S(t)$, $t > 0$ denotes the silver prices, μ and $\sigma > 0$ are drift (constant mean) and diffusion (constant volatility) coefficients, respectively, and the $B^H(t)$ is the fractional Brownian motion [4].

The model in Equation 4.1 is a fundamental stochastic differential equation used in many fields to explain the changes in the data as a function of time. The solution of this model is derived by using Ito's Lemma.

$Lemma$ 1. (Ito's Lemma) Let $S(t)$ be an Ito process satisfying

$$dS(t) = \mu(S(t), t)dt + \sigma(S(t), t)dB(t) \tag{4.2}$$

where μ and $\sigma > 0$ are drift and diffusion coefficients, respectively and $B(t)$ is the standard Brownian motion. And, let $f(s, t)$ be a twice-differentiable function; then

we have that f (S(t), t) an Ito process, and

$$d(f(S(t),t)) = \frac{\partial f(S(t),t)}{\partial t}dS(t) + f^{'}(S(t),t)dS + \frac{1}{2}f^{''}(S(t),t)dS(t)^2 \quad (4.3)$$

where $dS(t)^2$ is obtained by using the equalities $dt^2 = 0, dtdB_t = 0, dB_t^2 = dt$.

Now, applying Ito's Lemma, Lemma 1 with $f(t, S(t)) = ln(S(t))$ we obtain

$$\begin{aligned} d\ln(S(t)) &= f^{'}(S(t),t)dS + \frac{1}{2}f^{''}(S(t),t)S(t)^2\sigma^2 dt \\ &= \frac{1}{S(t)}(\sigma S(t)dB(t) + \mu S(t)dt) - \frac{1}{2}\sigma^2 dt \\ &= \sigma dB(t) + (\mu - \frac{\sigma^2}{2})dt \end{aligned} \quad (4.4)$$

Taking the integral of both sides from 0 to t, gives,

$$\ln(S(t)) = \ln(S(0)) + \sigma(B(t) - B(0)) + (\mu - \frac{\sigma^2}{2})t \quad (4.5)$$

Finally, exponentiating gives the expression for S,

$$S(t) = S(0)\exp(\sigma(B(t) - B(0)) + (\mu - \frac{\sigma^2}{2})t) \quad (4.6)$$

The model assumes that the diffusion process with deterministic drift and diffusion coefficients is followed by the natural logarithm of stock price $S(t)$, when $t > 0$. The assumption of independent increments in the regular formula, however, is still up for discussion. This study investigates the relationship between examining the behavior of the previous super-cycle and the long-term dependence of asset returns. This reliance is not sufficiently addressed by the Brownian motion-based model in Equation 4.2.

While a number of time series models are put out for making short-term forecasts, the study's main objective is to estimate when the most recent super-cycle will have ended, which is a more probabilistic idea than data-driven forecasting. When predictions should terminate and super-cycle completion be recognized, data-driven models may find it difficult to make that decision. To analyze probabilistic route characteristics and identify patterns, a stochastic process model is therefore advised.

Due to its dependent increments, fractional Brownian motion is well suited for representing dependence characteristics in real-world data, such as market prices. Utilizing the Black-Scholes equation with fractional Brownian motion, which was developed by Mandelbrot and Van Ness [3] and acknowledges long-range dependency in stock returns, is highlighted in a new article by Njomen and Djeutcha [35]. This article recommends replacing the Brownian component of the popular Geometric Brownian motion model with fractional Brownian motion.

Fractional Brownian motion, commonly known as fractional Gaussian noise, is an incremental process $Y = \{Y_k : k = 0; 1; ...\}$, with the following formula: $Y_k = B^H(k+1) - B^H(k)$. For each k in this process Y_k, the standard normal distribution is present, but there is (generally) no independence. The associated autocovariance function, γ, has the following structure

$$\gamma(k) = \frac{1}{2}[|k-1|^{2H} - 2|k|^{2H} + |k+1|^{2H}] \tag{4.7}$$

for $k \in Z$. By applying the Taylor expansion at the origin of the function $h(x) = (1-x)^{2H} - 2 + (1+x)^{2H}$ and noting that $\gamma(k) = \frac{1}{2}k^{2H}h(\frac{1}{k})$ for $k \geq 1$, and it is seen that

$$\gamma(k) \sim H(2H-1)k^{2H-2} \tag{4.8}$$

as $k \to \infty$. For $H = 0.5$, the process corresponds with the standard Brownian motion, while for $H > 0.5$, the fractional Brownian motion exhibits long-range dependency as $\sum_{k=0}^{\infty} \gamma(k) = \infty$ and it displays the short-range dependence property when $H < 0.5$.

Now, by these fractional Brownian motion properties, we suggest using the following model, given in Equation 4.9, in which the Brownian component $B(t)$ is replaced by the Black-Scholes model $B^H(t)$ to capture both the dependency property and the change in the data over time.

$$dS(t) = \mu S(t)dt + \sigma S(t)dB^H(t) \tag{4.9}$$

By the result Lemma 3 of [35], the solution of Equation 4.9 which describes the fluctuations in the price of the silver data is then,

$$S(t) = S(0)\exp(\mu t + \sigma(B^H(t) - B^H(0)) - \frac{1}{2}\sigma^2 t^{2H}) \tag{4.10}$$

This solution is derived following similar steps to obtain Equation 4.6 and by using the following Ito's formula used for fractional Brownian motion given in Lemma 2. $Lemma$ 2. (Fractional Ito's Formula) Let $H \in [0,1]$. Assume that $f(s,t) : R \times R \to C^{1,2}(R \times R)$ and the random variable $f(t, B_H(t))$, $\int_0^t \frac{\partial f}{\partial s}(s, B_H(s))ds$ and $\int_0^t \frac{\partial^2 f}{\partial s^2}(s, B_H(s))s^{2H-1}ds$ all belong to $L^2(P)$ then

$$d(f(S(t),t)) = \frac{\partial f}{\partial s}(s, B_H(s))ds + \frac{\partial f}{\partial x}(s, B_H(s))dB_H(s) + H\frac{\partial^2 f}{\partial x^2}(s, B_H(s))s^{2H-1}ds \tag{4.11}$$

Please refer to [28] for the proof.

Note that, while finding the solution of the model given in Equation 4.9, taking the integral from $t-1$ to t results in the solution,

$$S(t) = S(t-1)\exp\left(\mu + \sigma(B^H(t) - B^H(t-1)) - \frac{1}{2}\sigma^2\right) \tag{4.12}$$

where the increment $B^H(t) - B^H(t-1)$ has a standard normal distribution for every $t = 1, 2...$ The solutions set out in Equation 4.11 and 4.12 and the properties of the fractional Brownian motion suggest that when fitted to silver prices, the model, Equation 4.10, has the following assumptions:

1. The standardized log-returns of the silver price,

$$Z^1 = \frac{\ln S(t) - \ln S(0) - \overline{\mu}}{\overline{\sigma}} \tag{4.13}$$

   where $\overline{\mu} = \mu t - \frac{1}{2}\sigma^2 t^{2H}, \overline{\sigma} = \sigma t^H$ and

$$Z^2 = \frac{\ln S(t) - \ln S(t-1) - (\mu - \frac{1}{2}\sigma^2)}{\sigma} \tag{4.14}$$

   both follow standard normal distribution for all $t = 1, 2...$

2. The standardized log-returns of the silver price, Z^2 or the increment process $\ln(S_t) - \ln(S_{t-1})$ of the silver prices, assumed to have the stationary property in the usual sense however the increment process $\ln(S_t) - \ln(S_0)$ or Z^1 assumed to have the stationary property in the extended sense that is the distribution depends only on the length of the time interval, t.

3. The standardized log-returns of the silver price have dependence property explained through the Hurst index, H.

4.2 Assumption Check of fBm for Silver Prices

The following three fundamental assumptions should be verified when using the geometric fBm as modeling our data set, the historical silver prices.

1. Normality
2. Stationarity
3. Dependence of increments

To make sure that our proposed model matches the silver data well, we first check these assumptions. Whether the previous super-cycle has ended or not is the aim in this analysis. The data set's beginning month is January 2005. We take the price of S_0 equal to the average price of January 2005 and apply it to silver data from the year 2005 onwards. Using the data set, we first determine the values of the standardized log-returns Z^1 and Z^2 and validate the model's assumptions.

4.2.1 Normality

In order to check the normality of the standardized log-returns we perform the Jarque-Bera test in which the null hypothesis considers the standard normal distribution. When dealing with economics data, the histogram is also recommended for the visual check in Marathe and Ryan study of [31].

The hypothesis for this test is:

- H_0: Normal distribution is assumed.
- H_1: Normal distribution is not assumed.

The test's p-value is taken into consideration, and the null hypothesis cannot be rejected if the actual p-value is greater than the acceptable value of significance α.

Results:

We use $S(0)$, the starting price as the average price of silver in January 2005 to present the results of the Jarque-Bera test performed on the standardized log-returns provided in Equations 4.13 and 4.14. Figure 4.3 shows the histogram and test results of the Jarque-Bera test of the standardized log-returns both Z^1 and Z^2 of silver prices.

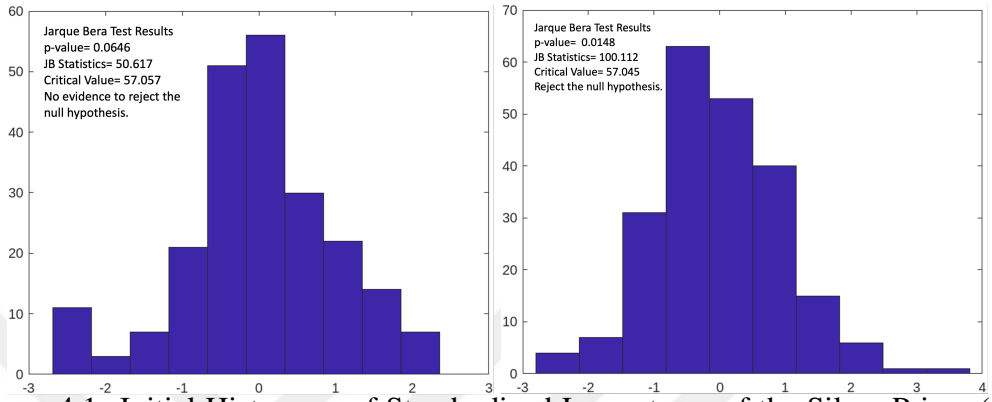


Figure 4.1: Initial Histogram of Standardized Log-returns of the Silver Prices (Z^1 - Z^2)

The standardized log-returns of $\ln(S_t) - \ln(S_0)$ is normally distributed with a 0.06 probability for Z^1 which is greater than p-value 0.05, as can be shown in Figure 4.3. However, the standardized log-returns of $\ln(S_t) - \ln(S_{t-1})$ beginning in January 2005 is not normally distributed with a 0.01 probability for Z^2, hence the model in Equation 4.9 does not apply to this data set. To achieve the normality for Z2, we applied HP filtering to the standardized log-returns of silver data in June 2006, February 2008, April 2008, August 2008, September 2009, September 2014, May 2020 and August 2020, depicted in Figure 4.4. We applied HP filter for the ones with big difference in the logarithmic returns of $\ln(S_t) - \ln(S_{t-1})$. Thus, we have transformed the extreme values in the distribution or the large-valued changes that occur in a short time into a more balanced one, and in particular, we have ensured that the distribution gets rid of its right bias. We preferred to smooth out returns at those times without losing generality because our major objective is to estimate whether the most recent super cycle is complete or not. The HP filter is used to keep the fluctuations coincident with the originals, ensuring that neither the start of the previous cycle nor the depth of the current cycle are altered.

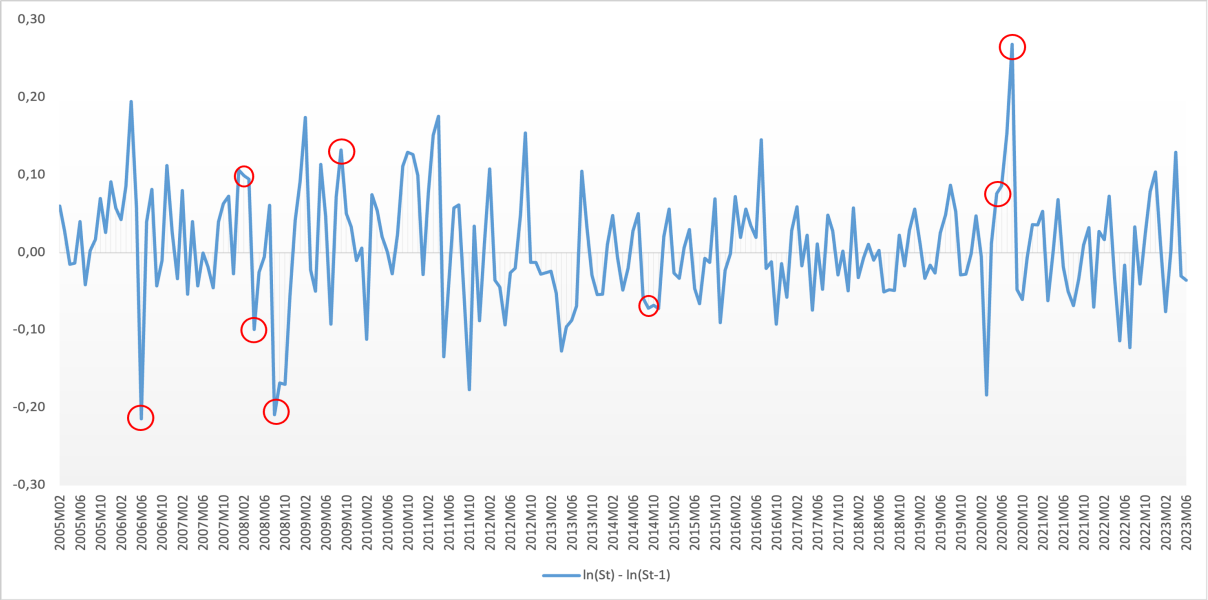


Figure 4.2: Points Applied HP Filter in Silver Price Data

As recommended for monthly pricing in economics data, [26], we use the filtering parameter $\lambda = 14400$. After applying the Normality test again we see that the Jarque-Bera test findings and histogram for the standardized smoothed log-returns of the silver prices which are depicted in Figure 4.7, imply that there is insufficient data to reject the standard Normal distribution as the null hypothesis. With a probability of 0.248 for Z^2 in the next normality test, the null hypothesis could not be rejected that the series are normally distributed. Therefore, the histogram and Jarque Bera normality tests confirm the data's normality.

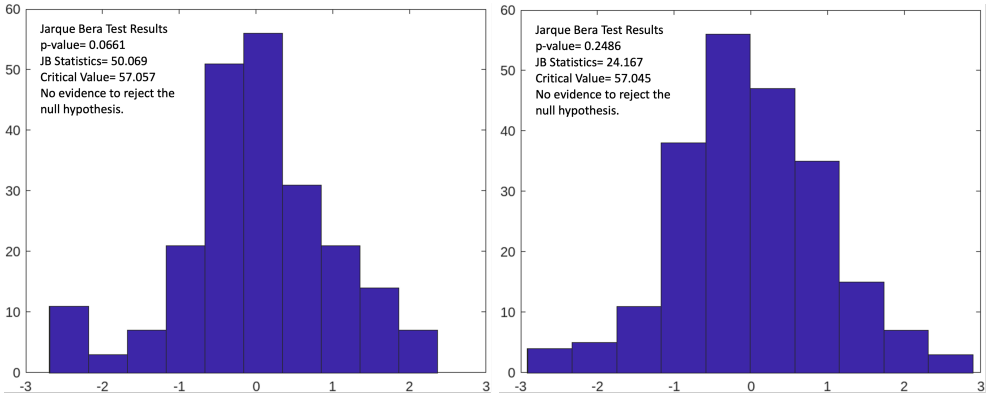


Figure 4.3: Final Histogram of Standardized Log-returns of the Silver Prices (Z^1 - Z^2)

4.2.2 Stationarity

The fractional Brownian model assumes stationarity for the increments from the smoothed data of the silver prices. The increment process $\ln(S_t) - \ln(S_{t-1})$ of the silver prices is assumed to be stationary in the usual sense, while the increment process $\ln(S_t) - \ln(S_0)$ is stationary in the extended sense, where the distribution only depends on the duration of the time interval, t.

If the statistical characteristics of the fBm process remain constant over time, it is stationary [23]. This presumption necessitates confirming that the fBm process' mean and covariance structure remain constant over the course of the observed time period.

The change in the smoothed increments $\ln(S_t) - \ln(S_{t-1})$, should be random in the case of the fractional Brownian motion model. In the event that this change is not random, the process is non-stationary and its variance rises with time t. Statistic tests like the Augmented Dickey-Fuller (ADF) test or the Kwiatkowski-Phillips-Schmidt-Shin (KPSS) test are frequently used to measure this stationarity [25].

KPSS test:

KPSS is one of the most effective tests for unit root. Unit root's presence indicates non-stationarity [25].

Its hypothesis is:

- H_0: Y_t is stationary.
- H_1: Y_t is not stationary (a unit root process).

If the KPSS test statistic is high, we conclude that the series is deviating from its mean and reject the null hypothesis.

The results of KPSS test applied to smoothed log-returns of the silver prices are as follows: KPSS test statistic is 0.1361, Critical Value is 0.146 and the p-value is 0.0683. These results indicate failure of the rejection of the null hypothesis, that

is the smoothed log-returns or smoothed increments, $\ln(S_t) - \ln(S_{t-1})$ of the silver prices are stationary.

Table 4.1: KPSS Test Results of $\ln(S_t) - \ln(S_{t-1})$

KPSS test statistic:	0.1361
Critical value:	0.146
p-value:	0.0683

ADF test:

ADF test is an additional well-known unit root test [11]. This test's hypotheses are presented in KPSS test's inverted sequence.

- H_0: Y_t is not stationary (a unit root process).
- H_1: Y_t is stationary.

Said and Dickey add to the standard Dickey-Fuller test to make it compatible with higher order ARMA(p,q) models [41].

The results of the ADF test of the smoothed increments $\ln(S_t) - \ln(S_{t-1})$ are as follows: ADF test statistics is -11.6735, Critical Value is -1.9422 and the p-value is 0.001. With these results we can reject the null hypothesis which is implying the stationarity of the standardized increments of the smoothed silver prices and conclude that the time series is stationary.

According to the proposed model given in Equation 4.13, $\ln(S_t) - \ln(S_0) \sim N(\overline{\mu}, \overline{\sigma})$ where $\overline{\mu} = \mu t - \frac{1}{2}\sigma^2 t^{2H}$ and $\overline{\sigma} = \sigma t^H$. The distribution of these log-returns $\ln(S_t) - \ln(S_0)$, therefore depends on the length of the time interval t, which is stationary in the general sense. To test the stationarity of these values using the standard tests referred above, we use the standardized smoothed log-returns $\ln(S_t) - \ln(S_0)$. Applying the ADF test on these standardized values we observe the following test results: ADF test statistics = -2.656 and Critical Value = -1.9422 and the p-value = 0.0083. These results indicate that the standardized log-returns of the silver prices $\ln(S_t) - \ln(S_0)$,

are stationary since the p-value is less than the significance level.

Table 4.2: ADF Test Results of $\ln(S_t) - \ln(S_0)$

ADF test statistic:	-2.656
Critical value:	-1.9422
p-value:	0.0083

4.2.3 Dependency

Investigating whether the increments are dependent is also crucial for verifying the fBm model's assumption. To find the relationship between the smoothed standardized log-returns of silver prices and the auto-correlation function and partial auto-correlation function, we use the serial correlations diagram. The correlogram is the finest descriptive graphic to test the serial correlation. For $k = 0, 1, 2, ..., M$, where $M < n$, serial correlations r_k vs the lag k are used to create a correlogram. However, it is difficult to anticipate independent observations for financial data. It is determined whether or not r_k falls within confidence limits when analyzing the dependency in the correlogram. Following is how these confidence intervals are set up:

$$-1/(n-1) \pm 1.96/\sqrt{n}$$

At the 5 percent level of significance, the correlation of series is significantly different from zero if there are enough auto-correlations and they are not within the standard error boundaries.

Results: The following is the hypothesis for the serial correlations:

- H_0: $\rho_0 = \rho_1 = ... = \rho_k = 0$ (There is no auto-correlation.)
- H_1: At least one is different.

Both Z^1 and Z^2 could be used to present the dependence however coinciding with the aim of the study Z^1 is the data set we will be using and simulating. Therefore, we prefer to work with the dependence structure of Z^1. The correlogram of the

auto-correlation and partial auto-correlation of Z^1 are illustrated for 20 lags in the following Figure 4.3. It is observed that there is obviously long range dependence in the data set, that is there is dependence in the data set. And, it is observed from the partial auto correlations that this long range dependence is mainly due to the data itself and highly correlated one step increments.

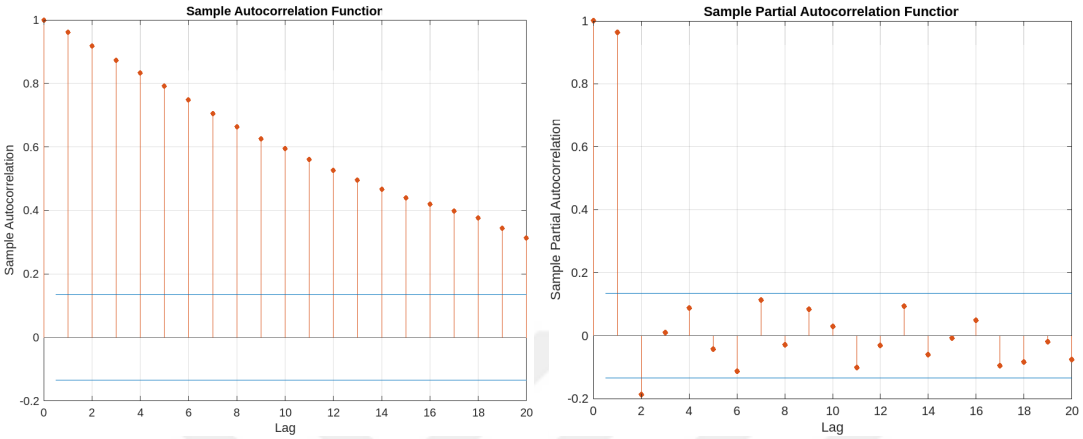


Figure 4.4: Correlation Diagrams

4.3 Estimation of H

We compute the Hurst parameter before and after the peak (April 2011) of silver prices to see if it changes with time, or to identify any non-stationarity caused by dependence. Using the data set, we first determined the values of the standardized log-returns and validated the model's assumptions. In order to do this, we divide the data into two parts, estimate the Hurst parameters for each part, then estimate the Hurst parameter for the full set of data. The Hurst parameter can be estimated using a variety of methods, including the R/S statistic [30], the variance-time estimator [49], the periodogram-based estimator [20], the Whittle maximum likelihood estimator [48], and the wavelet estimator.

The wavelet estimator and the Whittle maximum likelihood estimator were discovered to be the least biased when the Hurst parameter estimators were tested with regard to their bias and variances in the investigations of [28] and [22], The wavelet estimator also performs more quickly and with less computer complexity than the Whittle maximum likelihood estimator. As a consequence of these properties, we prefer to use the MATLAB-based Veitch and Abry wavelet estimate approach. This estimator is asymptotically unbiased and effective under the normality condition. We proceed with the models provided in Equations 4.10 and 4.13 in order to estimate the Hurst parameter, which explains the dependency structure in the data set, as there is no mention of the Hurst parameter in the model Equations 4.12 and 4.14. The standardized $\ln(S_t) - \ln(S_0)$ that is standardized log return, Z^1, has standard normal distribution. And for all $t > 0$,

$$\frac{\ln S(t) - \ln S(0) - \overline{\mu}}{\overline{\sigma}} \tag{4.15}$$

have the same distribution as $\frac{B_t^H}{t^H}$ as they follow the model given in Equation 4.10 and the distribution of B_t^H is centered Gaussian, each with variance t^{2H} for all $t \geq 0$. The complete data set, as well as the data sets for Equation 4.10 and Z^1 in Equation 4.13 divided into two, are all subjected to the Hurst estimate. The first section includes data up to September 2011, while the second section includes the rest of the data. September 2011 is taken into account because it is quite near to the peak value.

Table 4.3: Estimates of Hurst Parameter and 95 percent CIs

First half of the data up to September 2011:	0.759 [0.190 0.772]
Second half of the data starting with September 2011:	0.723 [0.585 0.763]
The entire data set:	0.732 [0.459 0.759]

Estimate of Hurst parameter for the first half is 0.759 and estimate of H for the second half is 0.723. They are very close to the estimate of entire data set which is 0.732. Estimate of H for entire data set is included in all confidence intervals. Therefore, we conclude that Hurst parameter's dependence structure in the data set is stationary. And, we can use the estimate of the Hurst parameter for entire data set in our simulation study.

$Remark$ The mean and standard deviation of the entire data set horizontally in time are taken into account when calculating the estimators of $\overline{\mu}$ and $\overline{\sigma}$. This is taken into account for a few factors. First, with only one path of historical data, it is impossible to estimate the randomness parameters at each time point; however, by standardizing with estimators of the complete data set, we already have observations from the standard Normal distribution. They can now be regarded as values from the standard normal distribution vertically. Second, it is clear from such standardization that the entire data set satisfies the assumptions of dependent stationarity and the other assumptions as well. Additionally, as will be discussed in the following chapter, this type of standardization is technically equivalent to the simulated values.

4.4 Simulation

We have checked all the assumptions of fractional Brownian motion model given in Equation 4.1 on smoothed Z^1 and Z^2. We further our work by conducting a simulation analysis of fractional Brownian motion using the widely known technique proposed by Abry and Sellan [1], implemented in Matlab, to ascertain whether or not the most recent super cycle has ended. We choose to carry on with the simulation research rather than come to analytical conclusions for the expected value of the highest possible increase and its time due to the recommended model's increments dependence characteristic. Theoretically, the predicted value of the highest possible increase for the fractional Brownian motion with $H = 0.5$ (i.e., when the increments are independent) is computed, and the well-known precise result is $\sqrt{\pi/2} \cong 1.253$ [12]. However, when there is dependence in the data set, as occurs when fractional Brownian motion with $H \neq 0.5$ is used as a model, only upper and lower limits for the expected value of the highest possible increase and the asymptotic distribution of the highest possible increase are available as analytical or theoretical expressions [44], [6].

The exact numbers of the expected highest possible increase and its duration for fractional Brownian motion cannot be calculated using the mathematical methods now in use. The closest values to the theoretical values have only ever been achieved by simulating fractional Brownian motion continuously and many times, collecting the values of the highest possible increase and related duration for each of these simulated fractional Brownian paths, and computing their mean. For this, we have generated 100,000 distinct fractional Brownian motion paths, each with 100000 steps. It is recommended in the literature to run at least 10,000 simulations and 10,000 steps in order to acquire accurate results for the expected highest possible increase of the Brownian motion; for further information, see [8]. We begin our simulation research by checking the method's accuracy before moving on. In order to do this, we simulate 100,000 iterations of fractional Brownian motion with $H = 0.5$ and each with 100,000 steps, and then we collect the results to see whether they match with the expected highest possible increase of the Brownian motion.

The expected highest possible increase values were obtained by repeating the procedure for a variety of Hurst parameter values, $H \neq 0.5$. Additionally, we saw that every conclusion fell within the parameters set forth by the theoretical research [44]. We were certain that our approach for the simulation research predicted the expected value of the highest possible increase and its length accurately with 100,000 simulations and 100,000 steps.

In order to estimate the Hurst parameter, which explains the dependence structure in the data set, we continue with the model given in Equation 4.10 and Equation 4.13, since there is no Hurst parameter appearing in the model Equation 4.12 and Equation 4.14. The standardized $\ln S(t) - \ln S(0)$ that is standardized log return, Z^1, has standard normal distribution. And for all $t > 0$,

$$\frac{\ln S(t) - \ln S(0) - \overline{\mu}}{\overline{\sigma}} \tag{4.16}$$

have the same distribution as $\frac{B^H}{t^H}$ as they follow the model given in Equation 4.10. Applying the Hurst estimation to the data sets of Equation 4.10 and Z^1, Equation 4.13, we observe the same values as the estimator of the Hurst exponent which is 0.732.

Now, the MATLAB code proposed by [1] generates fractional Brownian motion with increments having variance

$$V[B^H(t) - B^H(s)] = \sigma^2 |t - s|^{2H} \tag{4.17}$$

And using the Hurst parameter 0.732, we construct one hundred thousand fractional Brownian motions, each with one hundred thousand steps. For each path, we measure the highest possible increase's magnitude and its duration. The average value of the highest possible increases' magnitude and duration is then determined. Let's take a moment to review the scaling property of the fractional Brownian motion, which is a highly significant and helpful characteristic of our simulation research, before presenting the findings. The fractional Brownian motion is a stochastic process that possesses the scaling property, which can be interpreted as the scaling in time is same as the scaling in space, that is, for a fractional Brownian motion B_t^H and for any time

$t > 0$ and a constant $c > 0$,

$$(B_{ct}^H) \tag{4.18}$$

For a fractional Brownian motion with drift 0 and combining with the scaling property we have, for any time $t > 0$,

$$\begin{aligned} E(M_t^{H,+}) &= \sup_{0\le u\le v\le t}(B_v^H - B_u^H) \\ &= \sup_{0\le u\le t}(\overline{B}_u^H - B_u^H) = \sup_{0\le \frac{u}{t}\le 1}(\overline{B}_u^H - B_u^H) \\ &= \sup_{0\le u'\le 1}(\overline{B}_{u't}^H - B_{u't}^H) = t^H \sup_{0\le u'\le 1}(\overline{B}_{u'}^H - B_{u'}^H) \\ &= t^H M_1^{H,+} \end{aligned} \tag{4.19}$$

where $\overline{B}_u^H := sup_{0\le u\le v} B_u^H$. By the scaling property, for a process up to time t we also have,

$$\begin{aligned} \sigma_d^t &= inf\{0 \le u \le t : \overline{X}_u - X_u = d\} \\ \sigma_d^1 &= inf\{0 \le \frac{u}{t} \le 1 : \overline{X}_{\frac{u}{t}} - X_{\frac{u}{t}} = d'\} \end{aligned} \tag{4.20}$$

where $d' = \frac{d}{t}^H$. Thus, note that $\sigma_d^t = t\sigma_d^1$. And hence,

$$\begin{aligned} \kappa_{\sigma_d^t} &= inf\{0 \le s \le \sigma_d^t : \overline{X}_s - \overline{X}_{\sigma_d^t} = d\} \\ \kappa_{\sigma_d^1} &= inf\{0 \le \frac{s}{t} \le \sigma_d^1 : \overline{X}_{\frac{s}{t}} - \overline{X}_{\sigma_d^1} = d\} \end{aligned} \tag{4.21}$$

which results in the equality $K_{\sigma_d^t} = tK_{\sigma_d^1} =$. Therefore, by the scaling property, the duration of the maximum drawup has the following property,

$$\tau_d^t = \sigma_d^t - \kappa_{\sigma_d^t} = t\sigma_d^1 - t\kappa_{\sigma_d^t} = t\tau_d^1 \tag{4.22}$$

Under this proposed fractional Brownian motion model, through the simulation study, we aim to find the expected highest possible increase and its duration of log-returns of the simulated silver prices, $\ln S(t) - \ln S(0)$, to make comparisons with the real historical prices. In order to match the law of real prices with the simulated values first, we start by observing the mean and the standard deviation of the real prices. And continue with generating fractional Brownian motion, that is $B_t^H \sim N(0, t^H)$,

$t > 0$ using the implemented Matlab code and we standardize them. Afterwards, we multiply these generated values with the standard deviation and add the mean of the entire data set in order to rescale them to the space of the real values and to have the same distribution as these historical prices $\ln S(t) - \ln S(0)$. We use the entire data set estimators since there is stationarity in the whole data set in terms of distribution and dependency as shown in the stationarity assumption check in Section 4.2.2. In other words, the highest possible increase in this simulation study is identical in law with;

$$\begin{aligned} M_t^{H,+} &= \sup_{0\leq u\leq v\leq t}((\overline{\sigma}\frac{B_u^H}{u^H}+\overline{\mu})-(\overline{\sigma}\frac{B_v^H}{v^H}+\overline{\mu}) \\ &= \sup_{0\leq u\leq v\leq t}[(\ln S(u)-\ln S(0))-(\ln S(v)-\ln S(0))] \end{aligned} \tag{4.23}$$

where μ and σ, respectively, are estimators of the mean and standard deviation of the log-returns of the silver price. Using this sample mean and sample standard deviation to standardize past log-returns, we automatically detect values from the standard Normal distribution at each time point. The standardized nature of the path vertically in time is therefore implied by this. This is why, using simulation analysis, we are able to get $\frac{B_t^H}{t^H}$ values for each time point $t = 1, 2, ...$, identical in law, with the values of the standardized real log-returns. We bring the simulated values to the same scale as the historical log returns by rescaling them in space using the mean and standard deviation of real prices, and they likewise exhibit the same dependency structure. The expected highest possible increase and the expected duration of highest possible increase discovered by the simulation study thus match the expected highest possible increase and the expected duration of highest possible increase of the observations $\ln S(t) - \ln S(0)$, $t \geq 0$, as these observations are identical in law with the simulated values.

For comparison reasons, from the log-returns of the silver prices, we first observe the values of the highest possible increase and its duration of $\ln S(t) - \ln S(0)$ for $0 \leq t \leq 222$. The highest possible increase and its duration for this data set are observed respectively as 1.86 and 76. Additionally, by the simulation analysis, we are able to predict the maximum gain of standardized fractional Brownian motion up

to time 100000 steps as

$$E(M_{100000}^{0.732,+}) = 2.356$$

It should be noted that when fractional Brownian components B_t^H are substituted with the standardized rescaled fractional Brownian motion components $\overline{\sigma}\frac{B_t^H}{t^H} + \overline{\mu}$ used in Equation 4.23, the scaling property stated in Equation 4.19 still applies.Hence, by the scaling property, the expected value of the highest possible increase up to time 222 could be calculated from this result as follows;

$$E(M_{222}^{0.732,+}) = \frac{E(M_{100000}^{0.732,+})}{100000^H} = 222^{0.732}\frac{2.356}{100000^{0.732}} = 0.0269$$

Additionally, we have noted that the highest possible increase's expected time period for fractional Brownian motion up to time 100000 is

$$E(\tau_{M_{100000}^{0.732,+}}) = 71078$$

And after scaling this in time and determining the proportionate duration, we see that the highest possible increase's predicted length for fractional Brownian motion up to time 222 is equal to

$$E(\tau_{M_{222}^{0.732,+}}) = \frac{222}{100000}71078 = 157.8$$

The results of the simulation of the fractional Brownian motion (FBm) with H = 0.732 are summarized in Table 4.4 below. The fBm simulation results show that the expected duration of the highest possible increase is roughly 157 months, and the magnitude of the highest possible increase is close to 0.026 units. On the other hand, the highest drawup's duration is 76 months, and its size is around 1.86 units, according to the observed data.

Table 4.4: Comparison of the Simulation Study with the Actual Data Set for t=222, Hurst Parameter=0.732

	Expected value of fBm	Observed values
The Highest Possible Increase	0.0269	1.86
Duration of The Highest Possible Increase	157.8	76

Additionally, we calculated the maximum loss up to time 100000 steps as

$$E(M_{100000}^{0.732,-}) = 2.356$$

It has the same value with the highest possible increase as 2.356 and so the amount up to time 222 is the same.

$$E(M_{222}^{0.732,-}) = \frac{E(M_{100000}^{0.732,-})}{100000^H} = 222^{0.732}\frac{2.356}{100000^{0.732}} = 0.0269$$

The highest possible drop's expected time period for fractional Brownian motion up to time 100000 is calculated as

$$E(\tau_{M_{100000}^{0.732,-}}) = 41697$$

After scaling this in time we decided the expected duration of the highest possible drop up to time 222 is equal to

$$E(\tau_{M_{222}^{0.732,-}}) = \frac{222}{100000}41697 = 92.6$$

In the end we also have a simulation result for the highest possible drop and its duration shown in the following Table 4.5.

Table 4.5: The Highest Possible Drop Simulation for t=222, Hurst Parameter=0.732

	Expected value of fBm	Observed values
The Highest Possible Drop	0.0269	1.11
Duration of The Highest Possible Drop	92.6	133

4.5 The Model Validation

We work with silver prices that have been smoothed at values where there are jumps or outliers since, in our analysis, determining whether or not the most recent super cycle is complete is our main goal. The components of the jumps in the stochastic continuous-time model may be disregarded, according to this argument. As there is dependency in the log returns of the silver prices, which would undoubtedly have a significant impact on the fluctuations, our suggestion is to utilize fractional Brownian motion to characterize the evolution of the log returns. In order to demonstrate that our suggested model is elevated we compare the mean square errors (MSEs) of the Brownian motion and fractional Brownian motion models for log-returns of silver prices. The Monte Carlo MSE between the simulated prices and market prices is therefore calculated by simulating these continuous-time stochastic processes, which is done repeatedly. We produce a fractional Brownian motion that replicates $B_t^H \sim N(0, t^{2H})$, as explained in Section 4.4, standardize these values, and then rescale them in space using the estimators of the mean and standard deviation of the complete historical silver price log-returns, i.e. we produce $\overline{\sigma}\frac{B_t^H}{t^H} + \overline{\mu}$. Equation 4.6's proposed model generates the following results:

$$\overline{\sigma}\frac{B_t^H}{t^H} + \overline{\mu} = \ln S(t) - \ln S(0), t \geq 0$$

After that, we compare the mean square errors of the two models to show how the fractional Brownian motion model with $H = 0.732$ and the Brownian motion model with $H = 0.5$ compare to one another.

$$MSE = \frac{\sum_{j=1}^{N}(\frac{\sum_{i=1}^{L}(\overline{\sigma}\frac{B_i^H}{iH} + \overline{\mu} - \ln(S(i)))^2}{L})}{N}$$

where L and N stand for the number of lengths or steps and the amount of simulations, respectively. The following Table 4.6 displays the findings.

It can be observed that the geometric Brownian motion process has a larger mean square error than the fractional Brownian motion model when simulated sample pathways are compared to the price of silver. In light of this, we draw a conclusion that

Table 4.6: The Mean Square Errors

The Stochastic Model of log-returns	MSE
The fractional Brownian motion with H = 0.732	0.2702
The fractional Brownian motion with H = 0.5 (Brownian motion)	0.2709

the adoption of fractional Brownian motion as a model, which does actually give a progress in understanding the evolution of silver price log-returns.

CHAPTER 5

CONCLUSION

In this thesis, the goal was to determine the duration of super-cycle in silver prices by estimating the duration of the highest possible increase in silver prices, representing the longest period of price increase and the highest possible drop which is the longest period of price fall. The study is focused on World Bank silver price data, obtained from World Bank community prices website. The data covered the monthly period from January 2005 to June 2023. The silver prices data were modeled by GfBm.

The concept of the highest possible increase is significant for both investors and economists as it highlights the highest potential market gain. To identify the highest possible increase in the silver price data, the study employed the notion of super-cycles, which encompass upward and downward movements in the price series. Economic filtering method, Hodrick Prescott was used to extract these super-cycles by separating trend components and smoothing the data. By doing this, the last super-cycle was identified. This final super-cycle, found to have started around 2005 and peaked in 2011, determined the time interval used for modeling purposes.

In preparation for observing the results of the highest possible increase and its duration in both actual data and simulation studies, the study outlines the verification of the assumptions related to fractional Brownian motion (fBm) using real-life data.

Firstly, a histogram and the Jarque Bera normality test are applied to validate the normality of the differences in the logarithm of prices. Additionally, the stationarity of increments is examined, and both the KPSS and ADF tests confirm the stationarity of the series. Furthermore, the study establishes that the series exhibit correlation.

The study utilizes the geometric version of the fBm model to simulate silver prices. The fBm model is considered realistic due to its ability to portray long-term dependent behavior (when the Hurst parameter, H, is greater than 1/2), which corresponds to the dependency observed in real-life financial data. It's acknowledged in the literature that while Brownian motion captures the movements of silver prices, it fails to represent dependency. Therefore, fractional Brownian motion (fBm) is a more suitable replacement for Brownian motion in modeling the dependency observed in financial data.

For our dataset comprising 222 months of silver prices, the estimated Hurst parameter using the MATLAB-based Veitch and Abry wavelet estimate approach is approximately 0.7323. The Hurst parameter is a measure of the long-term dependence in a time series, where values above 0.5 indicate positive long-term dependence or persistence.

To analyze the fractional Brownian motion (fBm) and determine its highest possible increase and drop values, a simulation was performed. In this simulation, 100,000 paths were generated, each consisting of 100,000 steps. The goal was to estimate key parameters. The average of 100,000 highest possible increases and the average duration of them were calculated to provide an estimation. The simulation study employed the estimated Hurst parameter H = 0.7323 to model the behavior of the fBm in the analysis.

Utilizing the filtered silver price dataset, highest possible increase and highest possible drop and their corresponding durations were computed for the 222 observations. Consequently, the expected highest possible increase and duration of it for the filtered data amounted to 1.86 and 76, respectively. Conversely, the simulation outcomes for the highest possible increase and its duration at t = 222 were determined as 0.026 and 158, respectively. Moreover, the expected highest possible drop and duration of it for the filtered data amounted to 1.11 and 133. And simulation results for the highest possible drop and it duration at t = 222 were obtained as 0.026 and 93.

In light of these results, the expected duration of maximum gain as 158 and the du-

ration of maximum loss as 93, add up to 251 months which is the expected duration of the cycle. And according to the observed results, the cycle has ended at the 133rd month which is the duration of maximum loss. Therefore, when we take the durations into consideration, since 133 is less than 251, we can say the cycle has not been completed yet. However, when we evaluate the values, the cycle has ended at the 133rd month.

We revisit historical silver prices, starting in 1990, in an effort to draw more insightful conclusions. We suggest using the most recent maximum drop as a benchmark for a cycle started by the highest possible increase. On the other hand, with cycles that start from maximum decreases may be started analysis from the last highest point. Then, further studies may be carried out in accordance with this framework, producing comparisons that are more coherent. The use of other data sets in upcoming studies might give this conversation more depth.

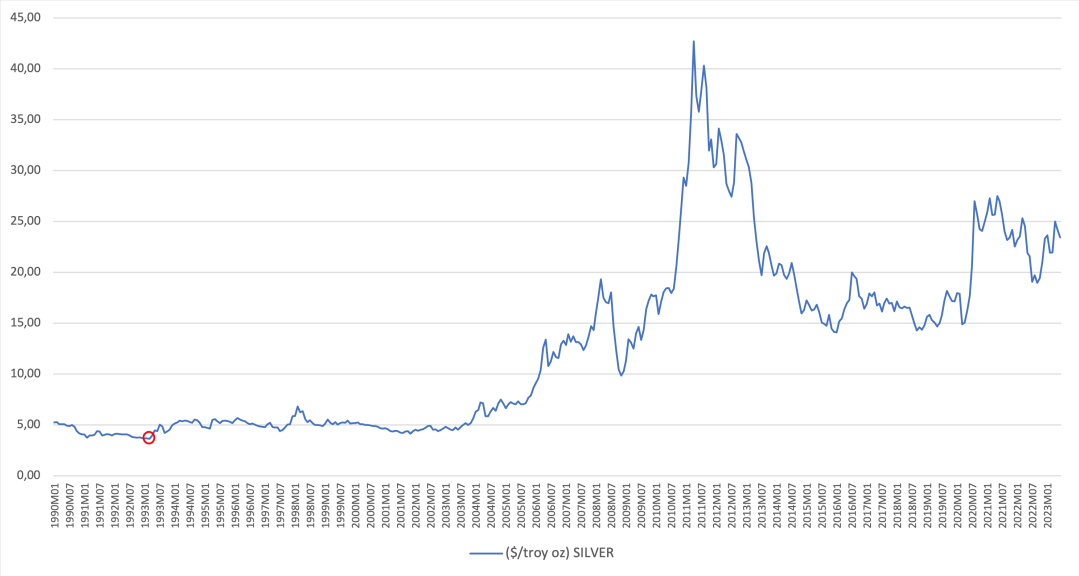


Figure 5.1: Silver Price Data: World Bank

The next conjectural approach is relevant to silver prices data set. We expect a drop in the Hurst parameter by going back in time to 1990s and starting the study from that point. By creating more independence among the data, this change would bring the data closer to Brownian motion. Notably, the data set's maximum value reaches its peak in 2011, while the most recent maximum drop is in 1993.

In this context, we find that the duration of the maximum increase has an observed value of 216 months, exceeding the expected duration of 158 months, see Table 4.4. This observation allows us to draw two conclusions: first, the highest possible increase has been achieved in terms of value and duration. Additionally, considering the symmetrical character of Brownian motion, we may deduce an ongoing trend in the downward movement. This conclusion suggests that the super-cycle is still ongoing and there are signs that it is about to come to an end.

REFERENCES

[1] ABRY, P., AND SELLAN, F. The wavelet-based synthesis for fractional brownian motion proposed by f. sellan and y. meyer: Remarks and fast implementation, 1996.

[2] A.L. ANDRÉ LUBENE RAMOS, D.B. MAZZINGHY, V. B., AND OLIVEIRA, M. Evaluation of an iron ore price forecast using a geometric brownian motion model. *REM - International Engineering Journal 72(1)* (2019), 9–15.

[3] B.B. MANDELBROT, J. V. N. Fractional brownian motions, fractional noises and applications. *Society for Industrial and Applied Mathematics 10(4)* (1968), 422–437.

[4] BIAGINI, F., HU, Y., ØKSENDAL, B., AND ZHANG, T. *Stochastic calculus for fractional Brownian motion and applications*. Springer Science & Business Media, 2008.

[5] BLACK, F., AND SCHOLES, M. The pricing of options and corporate liabilities. *Journal of Political Economy 81* (1973), 637–654.

[6] CAGLAR, M., AND VARDAR-ACAR, C. Distribution of maximum loss of fractional brownian motion with drift. *Statistics & Probability Letters 83*, 12 (2013), 2729–2734.

[7] CARRION-I SILVESTRE, J. L., AND SANSÓ, A. A guide to the computation of stationarity tests. *Empirical Economics 31*, 2 (2006), 433.

[8] CEREN VARDAR-ACAR, C. L. Z., AND SZÉKELY, G. J. On the correlation of the supremum and the infimum and of maximum gain and maximum loss of brownian motion with drift author links open overlay panel. *Journal of Computational and Applied Mathematics 248* (2013), 61–75.

[9] CHATFIELD, C. *The analysis of time series: an introduction*. CRC press, 2016.

[10] CHERIDITO, P. Arbitrage in fractional brownian motion models. *Finance and Stochastics 7(4)* (2003), 533–553.

[11] DICKEY, D. A., AND FULLER, W. A. Distribution of the estimators for autoregressive time series with a unit root. *Journal of the American statistical association 74*, 366a (1979), 427–431.

[12] DOUADY, R., SHIRYAEV, A. N., AND YOR, M. On probability characteristics of" downfalls" in a standard brownian motion. *Theory of Probability & Its Applications 44*, 1 (2000), 29–38.

[13] DUC KHUONG NGUYEN, T. W. Modeling and forecasting commodity market volatility with long-term economic and financial variables. *Journal of Forecasting* (2020), 126–142.

[14] EDMUNDO G DE SOUZA E SILVA, L. F. L., AND DE SOUZA E SILVA, E. A. Forecasting oil price trends using wavelets and hidden markov models. *Energy Economics 32(6)* (2010), 1507–1519.

[15] ERDEM, F. P., AND ÜNALMIŞ, İ. Revisiting super-cycles in commodity prices. *Central Bank Review 16*, 4 (2016), 137–142.

[16] ERTEN, B., AND OCAMPO, J. A. Super cycles of commodity prices since the mid-nineteenth century. *World Development 44* (2013), 14–30.

[17] ERYIGIT M., G. V. Modelling volatility of istanbul stock exchange national 100 index returns: Long memory vs. arima models. *Journal of Applied Statistics* (2018), 1575–1593.

[18] F.J. MOLZ, H.H. LIU, J. S. Fractional brownian motion and fractional gaussian noise in subsurface hydrology: A review, presentation of fundamental properties, and extensions. *Water Resources Research 33 (10)* (1997), 2273–2286.

[19] FULIŃSKI, A. Fractional brownian motions: memory, diffusion velocity, and correlation functions. *Journal of Physics A: Mathematical and Theoretical 50(5)* (2017).

[20] GEWEKE, J., AND PORTER-HUDAK, S. The estimation and application of long-memory time- series models. *Journal of Time Series Analysis 4* (1983), 221–238.

[21] GUASONI, P. No arbitrage under transaction costs, with fractional brownian motion and beyond. *Mathematical Finance 16(3)* (2006), 569–582.

[22] HAE-DUCK J JEONG, JONG-SUK R LEE, D. M., AND PAWLIKOWSKI, K. Comparison of various estimators in simulated fgn. *Simulation Modelling Practice and Theory 15(9)* (2007), 1173–1191.

[23] HAMILTON, J. D. *Time series analysis*, vol. 2. Princeton university press Princeton, NJ, 1994.

[24] HAMILTON, J. D. What's real about the business cycle? Tech. rep., National Bureau of Economic Research, 2005.

[25] HARRIS, R. I. Testing for unit roots using the augmented dickey-fuller test: Some issues relating to the size, power and the lag structure of the test. *Economics letters 38*, 4 (1992), 381–386.

[26] HODRICK, R. J., AND PRESCOTT, E. C. Postwar us business cycles: an empirical investigation. *Journal of Money, credit, and Banking* (1997), 1–16.

[27] HURST H. E., B. R., AND M., S. Y. *Long-term storage in reservoirs. An experimental study*. Constable, London, 1965.

[28] INKAYA, A. Option pricing with fractional brownian motion, 2011.

[29] J. CHAN, A. G. Modeling energy price dynamics: Garch versus stochastic volatility. *Energy Econ. 54* (2016), 182–189.

[30] MANDELBROT, B. B., AND WALLIS, J. R. Some long-run properties of geophysical records. *Water resources research 5*, 2 (1969), 321–340.

[31] MARATHE, R. R., AND RYAN, S. M. On the validity of the geometric brownian motion assumption. *The Engineering Economist 50*, 2 (2005), 159–192.

[32] MISIRAN M., L. Z., AND L., T. K. Fractional black-scholes models: complete mle with application to fractional option pricing. *International Conference on Optimization and Control* (2010), 573–586.

[33] MOHAMED AROURI, D. K. N. Oil prices, stock markets and portfolio investment: Evidence from sector analysis in europe over the last decade. *Energy Policy* (2010), 4528–4539.

[34] NILSSON, R., AND GYOMAI, G. Cycle extraction: A comparison of the phase-average trend method, the hodrick-prescott and christiano-fitzgerald filters. *OECD Statistics Working Papers*, 2011/4 (2011).

[35] NJOMEN, D. A. N., AND DJEUTCHA, E. Solving black-schole equation using standard fractional brownian motion. *Journal of Mathematics Research 11(2)* (2019), 142–157.

[36] PALLEY, T. I. A theory of minsky super-cycles and financial crises. *Contributions to Political Economy 30*, 1 (2011), 31–46.

[37] POSPISIL J., K. L. Fractional dynamics models of interest rates and stock prices. *Quantitative Finance* (2018), 1307–1319.

[38] QIANG LIANG, Y. F., AND WEI, Y. A long-term trend forecasting approach for oil price based on wavelet analysis. *Chinese Journal of Management Science 13(1)* (2005), 30–36.

[39] RAVN, M. O., AND UHLIG, H. On adjusting the hodrick-prescott filter for the frequency of observations. *Review of economics and statistics 84*, 2 (2002), 371–376.

[40] S. ROSTEK, R. S. A note on the use of fractional brownian motion for financial modeling. *Economic Modelling 30* (2013), 30–35.

[41] SAID, S. E., AND DICKEY, D. A. Testing for unit roots in autoregressive-moving average models of unknown order. *Biometrika 71*, 3 (1984), 599–607.

[42] THEU DINH, STÉPHANE GOUTTE, D. K. N., AND WALTHER, T. Economic drivers of volatility and correlation in precious metal markets. *Journal of Commodity Markets* (2022), 100242.

[43] T.N.T. NGUYEN, N. T. Methodology to forecast commodity prices in vietnam. *International Journal of Finance Economics 7* (2015), 44–49.

[44] VARDAR-ACAR, C., AND BULUT, H. Bounds on the expected value of maximum loss of fractional brownian motion. *Statistics & Probability Letters 104* (2015), 117–122.

[45] VEITCH, D., AND ABRY, P. A wavelet-based joint estimator of the parameters of long-range dependence. *IEEE Transactions on Information Theory 45(3)* (1999), 878–897.

[46] W. WILLINGER, M.S. TAQQU, R. S., AND WILSON, D. Self-similarity through high variability: statistical analysis of ethernet lan traffic at the source level. *IEEE/ACM Trans. Network. 5* (1997), 71–86.

[47] W.E. LELAND, M.S. TAQQU, W. W., AND WILSON, D. On the self-similar nature of ethernet traffic (extended version). *IEEE/ACM Trans. Network. 2* (1994), 1–15.

[48] WHITTLE, P. Estimation and information in stationary time-series. *Ark. Mat. 2* (1953), 423–434.

[49] ZHANG, H., SHU, Y., AND YANG, O. Estimation of hurst parameter by variance-time plots. In *Communications, Computers and Signal Processing, 1997. 10 Years PACRIM 1987-1997-Networking the Pacific Rim. 1997 IEEE Pacific Rim Conference on* (1997), vol. 2, IEEE, pp. 883–886.

[50] Z.N. HAMDAN, S.N.I. IBRAHIM, M. M. Modelling malaysian gold prices using geometric brownian motion model. *Advances in Mathematics: Scientific Journal 9 (9)* (2020), 7463–7469.

APPENDIX A

TABLES OF TIME SERIES

Table A.1: Hodrick-Prescott Filtering Results

Period	Silver Price	HP trend
2005-Month01	6.619	0.260157878421098
2005-Month02	7.03	0.245689754762129
2005-Month03	7.2282	0.231334810715848
2005-Month04	7.1188	0.217193347606745
2005-Month05	7.0224	0.203351532629168
2005-Month06	7.3105	0.189879391017866
2005-Month07	7.0145	0.176831879558659
2005-Month08	7.0334	0.164253561095695
2005-Month09	7.1536	0.152173848187339
2005-Month10	7.6705	0.140610933755441
2005-Month11	7.8725	0.129573619864063
2005-Month12	8.627	0.119065788795465
2006-Month01	9.1391	0.109084129793841
2006-Month02	9.5349	0.0996234192809734
2006-Month03	10.3838	0.0906748629121504
2006-Month04	12.6144	0.0822256922745827
2006-Month05	13.3772	0.0742627648780602
2006-Month06	10.7964	0.0667807414564624

Table A.2: Hodrick-Prescott Filtering Results-Cont.

Period	Silver Price	HP trend
2006-Month07	11.2324	0.0597732028812952
2006-Month08	12.1874	0.0532330260701503
2006-Month09	11.6769	0.0471516863094437
2006-Month10	11.5586	0.0415226288262797
2006-Month11	12.9311	0.0363330528903832
2006-Month12	13.2786	0.0315665671179104
2007-Month01	12.8413	0.0272120490459271
2007-Month02	13.91	0.0232580256480998
2007-Month03	13.1843	0.019688808674025
2007-Month04	13.7233	0.0164926462233719
2007-Month05	13.1478	0.0136526981953341
2007-Month06	13.1443	0.0111537616935616
2007-Month07	12.9093	0.00897671067086363
2007-Month08	12.3343	0.00710162602439928
2007-Month09	12.8335	0.0055067124753975
2007-Month10	13.6704	0.00416651741115698
2007-Month11	14.7016	0.00305796101257334
2007-Month12	14.3036	0.00216206120043791

Table A.3: Hodrick-Prescott Filtering Results-Cont.

Period	Silver Price	HP trend
2008-Month01	15.9089	0.00146467377463386
2008-Month02	17.569	0.000949598483741255
2008-Month03	19.3174	0.000607919991162658
2008-Month04	17.5	0.000430433183271928
2008-Month05	17.06	0.000414478942191874
2008-Month06	16.969	0.000556862477544169
2008-Month07	18.0339	0.000852591858824925
2008-Month08	14.635	0.0012962650684087
2008-Month09	12.373	0.00188664762881805
2008-Month10	10.4413	0.00262219586437132
2008-Month11	9.8652	0.00348957541268264
2008-Month12	10.2857	0.00446348178780215
2009-Month01	11.2682	0.00551442680529225
2009-Month02	13.4125	0.00661551100893192
2009-Month03	13.1168	0.00774578741412232
2009-Month04	12.4793	0.00889594702221686
2009-Month05	13.9838	0.0100545947898438
2009-Month06	14.6543	0.0112062579981641

Table A.4: Hodrick-Prescott Filtering Results-Cont.

Period	Silver Price	HP trend
2009-Month07	13.3617	0.0123426704318348
2009-Month08	14.3567	0.0134580400444711
2009-Month09	16.3895	0.0145393050624203
2009-Month10	17.2361	0.0155774569263788
2009-Month11	17.8213	0.0165637472239736
2009-Month12	17.6422	0.017491843353855
2010-Month01	17.749	0.0183565810898367
2010-Month02	15.873	0.0191508800630156
2010-Month03	17.1061	0.0198668042680901
2010-Month04	18.0623	0.0204873301647739
2010-Month05	18.4333	0.0209992500994604
2010-Month06	18.4548	0.0213917108933995
2010-Month07	17.9605	0.021653813025362
2010-Month08	18.3877	0.021773252389175
2010-Month09	20.5498	0.0217343357529613
2010-Month10	23.3933	0.0215214902881981
2010-Month11	26.5409	0.0211253539239984
2010-Month12	29.3248	0.020544069933764

Table A.5: Hodrick-Prescott Filtering Results-Cont.

Period	Silver Price	HP trend
2011-Month01	28.5086	0.0197830810304038
2011-Month02	30.7785	0.0188533301049557
2011-Month03	35.8135	0.0177624259610072
2011-Month04	42.6952	0.016521988323537
2011-Month05	37.3359	0.0151529248409303
2011-Month06	35.795	0.0136872014668585
2011-Month07	37.9171	0.0121464172038598
2011-Month08	40.3313	0.0105482936716334
2011-Month09	38.1545	0.0089137085705464
2011-Month10	31.9748	0.00726709358368077
2011-Month11	33.0818	0.00562840832156341
2011-Month12	30.3032	0.00400483720671859
2012-Month01	30.6509	0.00240553735481903
2012-Month02	34.1405	0.000833295409181579
2012-Month03	32.9532	-0.000708476766676866
2012-Month04	31.5255	-0.00220893751467751
2012-Month05	28.7196	-0.0036596540318105
2012-Month06	27.9836	-0.00505511592433048

Table A.6: Hodrick-Prescott Filtering Results-Cont.

Period	Silver Price	HP trend
2012-Month07	27.4318	-0.00639603205346535
2012-Month08	28.8002	-0.00768456309129652
2012-Month09	33.6085	-0.00892380857572897
2012-Month10	33.1874	-0.0101129538800653
2012-Month11	32.7732	-0.01123984267704
2012-Month12	31.8745	-0.0122924919568509
2013-Month01	31.06173913043	-0.0132590103301753
2013-Month02	30.3288	-0.0141285836506902
2013-Month03	28.79095238095	-0.0148912707233218
2013-Month04	25.355	-0.0155378074688978
2013-Month05	23.03826086957	-0.0160615093430418
2013-Month06	21.109	-0.0164634381505183
2013-Month07	19.7102173913	-0.016750194452343
2013-Month08	21.89386363636	-0.0169333089082756
2013-Month09	22.5638	-0.0170279102436851
2013-Month10	21.917	-0.0170406547841755
2013-Month11	20.7576	-0.0169749232745104
2013-Month12	19.67	-0.0168349328209797

Table A.7: Hodrick-Prescott Filtering Results-Cont.

Period	Silver Price	HP trend
2014-Month01	19.875	-0.0166274960315015
2014-Month02	20.845	-0.016361993769512
2014-Month03	20.716	-0.0160459322092685
2014-Month04	19.736	-0.015682372146934
2014-Month05	19.342	-0.0152736911724602
2014-Month06	19.892	-0.0148245432367148
2014-Month07	20.923	-0.0143399219982574
2014-Month08	19.736	-0.0138218444985086
2014-Month09	18.369	-0.0132678228265628
2014-Month10	17.163	-0.0126784650998914
2014-Month11	15.966	-0.0120545153013507
2014-Month12	16.295	-0.0114005528368599
2015-Month01	17.236	-0.0107253404406321
2015-Month02	16.787	-0.0100354326938316
2015-Month03	16.24	-0.00933274061874033
2015-Month04	16.341	-0.00862031134942642
2015-Month05	16.833	-0.0079028444298182
2015-Month06	16.075	-0.00718401021886584

Table A.8: Hodrick-Prescott Filtering Results-Cont.

Period	Silver Price	HP trend
2015-Month07	15.053	-0.00646487026976974
2015-Month08	14.941	-0.00574918696663963
2015-Month09	14.75	-0.00504483540837519
2015-Month10	15.813	-0.00435981006943463
2015-Month11	14.452	-0.0037026485627258
2015-Month12	14.127	-0.00307675314602983
2016-Month01	14.106	-0.00249151891912043
2016-Month02	15.167	-0.00195770682900808
2016-Month03	15.465	-0.00148600810757999
2016-Month04	16.36	-0.0010819418003961
2016-Month05	16.947	-0.000749572550295841
2016-Month06	17.286	-0.000488982926032696
2016-Month07	19.992	-0.000297755422166593
2016-Month08	19.587	-0.000172063152615434
2016-Month09	19.357	-9.79588824343167E-05
2016-Month10	17.655	-0.000062904685671911
2016-Month11	17.407	-5.51761093509675E-05
2016-Month12	16.432	-6.94356572371107E-05

Table A.9: Hodrick-Prescott Filtering Results-Cont.

Period	Silver Price	HP trend
2017-Month01	16.902	-0.000101324404561273
2017-Month02	17.933	-0.000150481505396548
2017-Month03	17.631	-0.000214580653445151
2017-Month04	18.033	-0.000287173242801701
2017-Month05	16.745	-0.00036297520186736
2017-Month06	16.931	-0.000435116912538476
2017-Month07	16.152	-0.000501849640827863
2017-Month08	16.952	-0.000560627314428024
2017-Month09	17.432	-0.000612140008982486
2017-Month10	16.941	-0.000653681788518811
2017-Month11	16.977	-0.000680565195072524
2017-Month12	16.165	-0.000690041464880195
2018-Month01	17.127	-0.000679167158298894
2018-Month02	16.582	-0.000648354463059735
2018-Month03	16.473	-0.00059395397511389
2018-Month04	16.648	-0.000514516987738448
2018-Month05	16.49	-0.000409011539957305
2018-Month06	16.541	-0.000275636092383647

Table A.10: Hodrick-Prescott Filtering Results-Cont.

Period	Silver Price	HP trend
2018-Month07	15.723	-0.000113222920976485
2018-Month08	14.987	7.96292848871815E-05
2018-Month09	14.272	0.000300807647229591
2018-Month10	14.597	0.000544864490912553
2018-Month11	14.353	0.000802936558126182
2018-Month12	14.772	0.00106768639577031
2019-Month01	15.624	0.00133055016288938
2019-Month02	15.815	0.00158488810401434
2019-Month03	15.296	0.00182786214051092
2019-Month04	15.055	0.00205736792812538
2019-Month05	14.662	0.00226885700020192
2019-Month06	15.036	0.00245653515659147
2019-Month07	15.791	0.0026126137592191
2019-Month08	17.224	0.00273088275874206
2019-Month09	18.16	0.0028083529542915
2019-Month10	17.645	0.00284787769498593
2019-Month11	17.165	0.00285579013967702
2019-Month12	17.138	0.00283622783653995

Table A.11: Hodrick-Prescott Filtering Results-Cont.

Period	Silver Price	HP trend
2020-Month01	17.972	0.00279121473511399
2020-Month02	17.88	0.00272246850476487
2020-Month03	14.884	0.00263481275626288
2020-Month04	15.065	0.00253252563579723
2020-Month05	16.256	0.00240696648594484
2020-Month06	17.713	0.0022501581795925
2020-Month07	20.647	0.00205484462417825
2020-Month08	27.003	0.00181957435239671
2020-Month09	25.742	0.00155339703253333
2020-Month10	24.23	0.00126595933239331
2020-Month11	24.079	0.000963478928896497
2020-Month12	24.968	0.000647881948703666
2021-Month01	25.88	0.000320593482196532
2021-Month02	27.293	-1.44886697098054E-05
2021-Month03	25.648	-0.000350997617823718
2021-Month04	25.687	-0.000678873814752689
2021-Month05	27.504	-0.000992350328768838
2021-Month06	26.995	-0.0012855075680544

Table A.12: Hodrick-Prescott Filtering Results-Cont.

Period	Silver Price	HP trend
2021-Month07	25.677	-0.00154761074831782
2021-Month08	23.986	-0.00176913302119827
2021-Month09	23.185	-0.00194391617745672
2021-Month10	23.413	-0.0020704100765859
2021-Month11	24.175	-0.00214928825118885
2021-Month12	22.532	-0.00218040087859857
2022-Month01	23.158	-0.00216122473990255
2022-Month02	23.542	-0.00209397287448193
2022-Month03	25.314	-0.00197880519693329
2022-Month04	24.545	-0.00181459413993136
2022-Month05	21.905	-0.00159503502868026
2022-Month06	21.556	-0.00131583949676745
2022-Month07	19.075	-0.000980510720225906
2022-Month08	19.724	-0.000593575825206527
2022-Month09	18.944	-0.000167985209539404
2022-Month10	19.426	0.000285675393321521
2022-Month11	21.018	0.00075402990794656
2022-Month12	23.326	0.00122542722007861
2023-Month01	23.653	0.00169363377161024
2023-Month02	21.921	0.00215956628065663
2023-Month03	21.976	0.00262499061149591
2023-Month04	25.01	0.00308624176440688
2023-Month05	24.267	0.00353964646721723
2023-Month06	23.417	0.00399029801402771